Facultad de Ciencias
Sección de Física

TRABAJO DE FIN DE GRADO

Ab initio studies on the electronic structure of atoms

Pablo Martínez Martínez

Project supervisors:
Dr. Javier Hernández Rojas
Dr. José Diego Bretón Peña

Departamento de Física

Date of submission: 10^{th} June 2021

I would like to thank my supervisors for the dedication, discussions and suggestions offered throughout the entirety of the project as well as my parents, Pedro and Lourdes, for their support at all the stages of this journey.

Table of contents

List of Tables **4**

List of Figures **4**

1 Summary **5**

2 Introduction **6**

3 Theoretical Background **7**
3.1 The atomic Hamiltonian 7
3.2 Electronic energy. Methods 9
3.2.1 Hartree-Fock self-consistent method 10
3.2.2 Møller-Plesset perturbation theory. Second-order corrections: MP2 . 11
3.3 Basis sets 13

4 NWChem **17**
4.1 Input file structure 18

5 Results and discussion **19**
5.1 HF calculations for light atoms 21
5.1.1 HF ground-state energies 21
5.1.2 Ionization energies 24
5.2 Extension to heavier atoms. MP2 refinement 25
5.2.1 Transition metals 29
5.3 Electron affinities 34

6 Conclusions **37**

References **40**

Appendix A Sample input file and data retrieval **41**

Appendix B Additional tables **42**

List of Tables

1 Spin-constrained ground-state energies for $Z \leq 10$ atoms and 1^{st} positive ions . . . 21
2 Study on the ground-state spin multiplicities for Sc-Zn . . . 30
3 Comparison between the expected, computational and reference values for the spin multiplicity of the 4^{th}-period transition elements . . . 31
4 Comparative view of ionic and atomic energies for the 6-311g* and cc-pvdz basis sets and their diffuse expansion for $Z = 9$. . . . 35
5 Comparison of the ground-state energy for alkalies using correlation and polarization consistent basis sets . . . 36
6 DFT estimation for the Sc and Ti ionization energies . . . 38
7 Electronic configurations and spin multiplicities for H-Kr as well as their first cations and anions . . . 39
8 HF and MP2 ground-state energies for atoms and cations H-Kr as well as their predicted ionization energies . . . 42
9 HF and MP2 electron affinities for atoms H-Kr . . . 42

List of Figures

1 Spatial distribution of cartesian GTOs for $l \in \{0, 1, 2\}$ . . . 15
2 Monoelectronic orbital diagram for the ground state of $Z \leq 10$ atoms . . . 22
3 Radial electron densities for $Z \leq 10$ atomic ground states . . . 23
4 Comparative view of radial electron densities for $Z \leq 10$ atomic ground states . . . 24
5 First ionization energy for atoms with $Z \leq 10$ and relative error . . . 25
6 First ionization energy for atoms with $1 \leq Z \leq 20$ and $30 \leq Z \leq 36$ and relative error for HF and MP2 correction . . . 26
7 Monoelectronic orbital diagram for the ground state of $11 \leq Z \leq 18$ atoms . 26
8 Monoelectronic orbital diagram for the ground state of K-Ca and Ga-Kr atoms . . . 27
9 Radial electron densities for $11 \leq Z \leq 18$ atomic ground states . . . 28
10 Ionization energies for $21 \leq Z \leq 30$ atoms assuming the $n + l$ and Hund's rule hold . . . 29
11 Ionization energies for $21 \leq Z \leq 30$ atoms after the spin multiplicity correction . . . 31
12 Monoelectronic orbital diagram for the ground state of $21 \leq Z \leq 30$ atoms . 32
13 Monoelectronic orbital binding energy dependence on the n and l quantum numbers . . . 34
14 Electron affinities for s and p-valence orbitals and relative error . . . 35
15 Electron affinities for $21 \leq Z \leq 30$ . . . 37

1 Summary

Este trabajo constituye un estudio teórico-computacional desde primeros principios de la estructura electrónica a un nivel atómico no relativista, a la par que introduce métodos teóricos generales de aplicabilidad en sistemas no solo atómicos sino también moleculares. En particular, se describen el método del campo autoconsistente de Hartree-Fock (HF) y la teoría de perturbación de muchos cuerpos desarrollada por Chr. Moeller y M. S. Plesset (MPN) hasta segundo orden (MP2).

El método HF define la energía del estado fundamental como un funcional de la función de onda del sistema, que es escogida como la antisimetrización del producto de funciones de onda monoelectrónicas. Estas funciones dependen de unos ciertos parámetros que son optimizados. Sin embargo, el formalismo de HF no estima la correlación electrónica, sino que recurre a un campo medio para estimar la interacción electrostática entre estas partículas. En este contexto se han desarrollado numerosos métodos post-HF a fin de estimar esta corrección a la energía del estado fundamental, entre los que se encuentra la teoría MPN.

Dada la naturaleza iterativa de estos métodos teóricos, se precisa de paquetes informáticos de química computacional para llevar a cabo los cálculos en casos prácticos. En este proyecto se ha hecho uso del paquete NWChem, siendo esta la primera ocasión en la Universidad de La Laguna que es empleado para cálculos atómicos. En la Sección 4 se incluye una breve introducción a su sintaxis y se adjunta un fichero ejemplo en el Apéndice A. Además, se discute en profundidad el formalismo de las bases de funciones de onda y sus familias principales en el contexto de la química computacional.

Siguiendo esta metodología, se ha resuelto la estructura electrónica de los átomos correspondientes a los cuatro primeros periodos de la tabla periódica (H-Kr) y se han contrastado las predicciones para las energías de ionización y afinidades electrónicas, dando muy buenos resultados y confirmando las configuraciones subyacentes.

La simulación de la estructura electrónica de los metales de transición del 4^{to} periodo (Sc-Zn) ha presentado serias dificultades, por lo que no se ha podido confirmar con nuestros cálculos la estructura electrónica de los aniones. Atribuimos estas complicaciones al alto número de orbitales disponibles con energías similares. Además, para átomos más pesados, el término de interacción de spin-órbita puede ser crucial en la determinación de las energías de los niveles monoelectrónicos. A pesar de ello, se ha podido resolver la estructura electrónica de los la mayoría de los átomos y de sus primeros cationes. Los átomos de Sc y Ti son especialmente sensibles a la elección de la base y no es posible asegurar su configuración electrónica. No obstante, un cálculo basado en el funcional de la densidad electrónica (DFT) también realizado con NWChem ha permitido estimar su configuración, si bien este proyecto no pretende ahondar en esta metodología en particular.

Por otro lado, se discute la exactitud de la aproximación del campo central, que propone una descripción complementaria de los sistemas polielectrónicos. La comparación entre la estructura predicha por la aproximación del campo central y los resultados computacionales permite justificar las reglas y postulados tales como las reglas de Hund de orden energético y el establecimiento de un principio de llenado (*Aufbauprinzip*) con un orden establecido. Nuestros cálculos han conducido a diferencias en el orden de

"llenado" con respecto al previsto teóricamente para los elementos de transición (Sc-Zn) y se ha observado una alta dependencia con la base escogida. También se ha podido constatar una preferencia por la ocupación de los orbitales en el orden $3d \rightarrow 4s \rightarrow 4p$ para los cálculos HF. La excepción a esta norma la encontramos en el Sc, donde las energías de los orbitales ocupados $4s$ y $3d$ son aproximadamente iguales. Precisamente este elemento y el siguiente (Ti) son los que han presentado más dificultades en el estudio. La diferencia de energía entre estos dos niveles se acrecienta al aumentar el número de electrones del sistema hasta tal punto que la subcapa $4s$ cede un electrón a la $3d$ para los átomos Fe-Cu.

Los resultados también evidencian una periodicidad en los valores numéricos de las afinidades electrónicas y energías de ionización, justificando así por métodos computacionales la ordenación de los elementos en grupos y periodos en la tabla periódica.

Por último, ha sido posible evaluar la densidad de probabilidad electrónica radial de estos elementos a partir de los orbitales HF. Si bien los métodos DFT son los más indicados para su cálculo, esta representación aproximada permite conectar la estructura energética de niveles ocupados con la probabilidad de presencia radial dentro del marco teórico del trabajo.

2 Introduction

The atomic hypothesis is arguably the most important discovery that science has brought to humanity from a fundamental perspective. In the words of Richard Feynman, Physics Nobel Prize laureate in 1965:

> "If, in some cataclysm, all of scientific knowledge were to be destroyed, and only one sentence passed on to the next generations of creatures, what statement would contain the most information in the fewest words? I believe it is the atomic hypothesis (or the atomic fact, or whatever you wish to call it) that all things are made of atoms—little particles that move around in perpetual motion, attracting each other when they are a little distance apart, but repelling upon being squeezed into one another. In that one sentence, you will see, there is an enormous amount of information about the world, if just a little imagination and thinking are applied."
>
> Richard Feynman, *The Feynman Lectures on Physics, Vol. I Ch. 1*

Indeed, this simple notion to our present eyes conveys an uncomplicated and yet extremely solid foundation to better understand or to at least make an educated guess on how matter behaves.

It has been known since the XIX century that every chemical species has a unique fingerprint in the form of emission or absorption spectra. Nowadays, we are acquainted with the fact that these spectral lines originate from electronic transitions between atomic or molecular energy levels. This knowledge about the atomic structure is at the core of many areas including fluorescence studies, laser design or material science.

Theoretical studies are nonetheless extremely valuable for industrial purposes as drug design for instance. The prediction and subsequent simulation of any system of interest allow to shed light on it as a whole rather than following an obscure trial and error procedure. This work intends to introduce the reader to some of the most common algorithms in computational chemistry used to simulate the electronic structure of any chemical species from first principles.

We shall restrict ourselves to the non-relativistic atomic domain, although the theory applies to molecular systems under the Born-Oppenheimer approximation. Section 3 will cover the fundamentals of the Hartree-Fock method as well as the second-order many-body perturbation theory of Chr. Moller and M. S. Plesset. Brief comments on the density functional theory will also be included in the conclusions so as to improve some computational results.

These methods are iterative-based and cannot be computed manually if a reasonable level of accuracy is demanded. Therefore, a computational chemistry package was needed to carry the calculations out. Chapter 4 is devoted to briefly describe the functioning of NWChem, a molecular-oriented software that will be adapted to atomic systems for the first time in the Universidad de La Laguna.

Finally, these theories will be applied in an attempt to unravel the electronic structure for atoms ranging from H to Kr. These results will be justified by direct comparison to experimental data for the ionization energies and the electron affinities. Furthermore, the results will be linked to qualitative predictions and principles regarding the mean-field approximation and the existence of an orbital filling principle. The computational results allow justifying their accuracy while also establish exceptions to these general statements.

In addition, Python programs have also been developed to produce the monoelectronic level diagrams shown in Figures 2, 7, 8 and 12 and the radial electron density plots of Figures 3, 4 and 9 based on the computational data.

3 Theoretical Background

En esta sección se discuten la naturaleza del problema físico planteado así como el formalismo mecano-cuántico empleado para su estudio. Tras esta introducción general, se describen los métodos teóricos que permiten un análisis cuantitativo de las energías (HF y MP2) de los estados fundamentales. Además, se discuten en profundidad las bases empleadas en cálculos *ab initio* en el contexto de la química computacional así como su función en la construcción y optimización de los orbitales electrónicos.

3.1 The atomic Hamiltonian

One of the basic magnitudes that *ab initio* methods allow estimating is the total energy of the system. We will tackle this problem as a general set of interacting particles without restricting it to the atomic domain yet. Both electrons and nuclei will be thought of as point-like particles in interaction without any internal degrees of freedom associated with their inner structure apart from the electron spin. We will consider that the total number

of particles is D.

This study will make use of the quantum-mechanical formalism so we will be working on the Hilbert space ϵ_T associated with the total system. This ϵ_T space is the tensor product of the individual Hilbert spaces of each particle:

$$\epsilon_T = \epsilon_1 \otimes \epsilon_2 \otimes ... \otimes \epsilon_D \quad , \tag{3.1}$$

where ϵ_i denotes the Hilbert space associated to the particle i. Assuming that the total wave function of the system is an eigenstate of the Hamiltonian operator $\hat{\mathcal{H}}$ of the total system, the energy of that state will be given by its eigenvalue under the Hamiltonian operation:

$$\hat{\mathcal{H}} \left|\Psi_n^{(\gamma)}\right\rangle = E_n^{(\gamma)} \left|\Psi_n^{(\gamma)}\right\rangle \quad . \tag{3.2}$$

In this notation, it is assumed that the energy spectrum is discrete, labelling the different eigenvalues with a subscript E_n. The possibility that the energy level is degenerate in the energy E_n is left open, for which a superscript $E_n^{(\gamma)}$ is added to distinguish those eigenstates from each other.

The Hamiltonian $\hat{\mathcal{H}}$ must include the kinetic energy of each particle and any interactions between them. Here, we will restrict the study to the non-relativist domain and therefore, the only significant interaction will be the electrostatic force. With this information, we write the most general expression for $\hat{\mathcal{H}}$ in the laboratory frame (LAB) as:

$$\hat{\mathcal{H}}_{LAB} = \sum_i^D \frac{\hat{\mathcal{P}}_i^{\,2}}{2m_i} + \frac{1}{2} \sum_{\substack{i,j \\ i \neq j}}^D \frac{q_i q_j}{4\pi\varepsilon_0 \hat{r}_{ij}} \quad , \tag{3.3}$$

where the first term is the total kinetic energy and the second term is the sum of potential energies for each i-particle as a result of their interaction with the j-particle. The division by 2 in (3.3) is necessary to not count the same interaction twice. The operator appearing in the electrostatic term is the module of the difference between the position operators of the particles[1] i and j:

$$\hat{r}_{ij} = |\hat{\mathbf{R}}_j - \hat{\mathbf{R}}_i| \quad . \tag{3.4}$$

This Hamiltonian is non-relativistic, which should be accounted for when judging the predicted results.

Now, we shift our attention to the atomic system in particular, where we will be dealing with one nucleus and N electrons. Particularizing the general Hamiltonian (3.3) results in:

[1] We note here that with particle i and j we are not labelling the electrons but rather the Hilbert Space H_i or H_j on which the action of the operators is defined.

$$\hat{\mathcal{H}}_{at}(\hat{\mathbf{P}}_A, \{\hat{\mathbf{P}}_i\}, \hat{\mathbf{R}}_A, \{\hat{\mathbf{R}}_i\}) = \frac{\hat{\mathcal{P}}_A^{\,2}}{2M_A} + \sum_i^N \frac{\hat{\mathcal{P}}_i^{\,2}}{2m_i} - \sum_i^N \frac{Z_A e}{4\pi\varepsilon_0 \hat{r}_{Ai}} + \frac{1}{2}\sum_{\substack{i,j \\ i\neq j}}^N \frac{e^2}{4\pi\varepsilon_0 \hat{r}_{ij}} \quad , \tag{3.5}$$

where the nuclear variables have been assigned the subscript "$_A$", e is the absolute value of the electron charge and Z_A the nucleus atomic number. It is convenient to change the reference system from LAB to the center of mass of the system (CM) through a canonical transformation $\left\{\hat{\mathbf{P}}_A, \{\hat{\mathbf{P}}_i\}, \hat{\mathbf{R}}_A, \{\hat{\mathbf{R}}_i\}\right\} \longrightarrow \left\{\hat{\mathbf{P}}_{CM}, \{\hat{\mathbf{p}}_i\}, \hat{\mathbf{R}}_{CM}, \{\hat{\mathbf{r}}_i\}\right\}$. The lower case position vectors $\{\hat{\mathbf{r}}_i\}$ stand for the electron position in the CM reference frame system while $\{\hat{\mathbf{p}}_i\}$ refer to their conjugate momenta. The new Hamiltonian is written as (we will remove the subscript $\hat{\mathcal{H}}_{at}$):

$$\hat{\mathcal{H}}(\hat{\mathbf{P}}_{CM}, \{\hat{\mathbf{p}}_i\}, \hat{\mathbf{R}}_{CM}, \{\hat{\mathbf{r}}_i\}) = \frac{\hat{\mathcal{P}}_{CM}^{\,2}}{2(M_A + Nm_e)} + \sum_i^N \frac{\hat{p}_i^{\,2}}{2m_e} + \sum_{i,j}^N \frac{\hat{\mathbf{p}}_i \cdot \hat{\mathbf{p}}_j}{2M_A} - \sum_i^N \frac{Z_A e}{4\pi\varepsilon_0 \hat{r}_{Ai}} + \frac{1}{2}\sum_{\substack{i,j \\ i\neq j}}^N \frac{e^2}{4\pi\varepsilon_0 \hat{r_{ij}}} \quad . \tag{3.6}$$

This expression separates the motion of the center of mass from the relative or internal movement. We will only study the internal part as the other is just a plane-wave solution that can be multiplied by the internal wave function. Lastly, the nucleus will be considered to have a mass much larger than the electrons, tending to infinity. Therefore, $\hat{\mathbf{R}}_{CM} = \hat{\mathbf{R}}_A$ and the mass polarization term[2] can be neglected to rewrite the expression as:

$$\hat{\mathcal{H}}(\{\hat{\mathbf{p}}_i\}, \{\hat{\mathbf{r}}_i\}) = \sum_i^N \frac{\hat{p}_i^{\,2}}{2m_e} - \sum_i^N \frac{Z_A e^2}{4\pi\varepsilon_0 \hat{r}_i} + \frac{1}{2}\sum_{\substack{i,j \\ i\neq j}}^N \frac{e^2}{4\pi\varepsilon_0 \hat{r_{ij}}} \quad . \tag{3.7}$$

Note on Eq. (3.7): the first and second terms on the right-hand side are usually called the one-electron Hamiltonian $\hat{h}_1$ while the last one is referred to as the two-electron Hamiltonian $\hat{h}_2$.

3.2 Electronic energy. Methods

Once the Hamiltonian operator (3.7) is defined, we must solve the eigenvalues equation (3.2), for which the system's wave function $|\Psi\rangle$ is needed. An analytical solution cannot be obtained for atoms with $N > 1$, as the electrostatic potential is not central due to the electronic repulsion. In order to determine the wave function and the energy associated, we will make use of the Hartree-Fock theory, which is described in the following section.

[2]The third term on the right-hand side of (3.6) $\sum_{i,j}^N \frac{\hat{\mathbf{p}}_i \cdot \hat{\mathbf{p}}_j}{2M_A}$ is the mass polarization term. Its order of magnitude is less than the fine structure of the atom, so its omission is justified for the precision depth of this work but should be accounted for hyperfine corrections.

3.2.1 Hartree-Fock self-consistent method

This method attempts to obtain the ground-state energy, i.e. the lowest, of the multi-electron system through a variational approximation. The trial wave function is written as a Slater determinant of monoelectronic functions called spin-orbitals, which we require to be orthonormal without loss of generality. This configuration allows the electronic wave function to be antisymmetric according to the spin-statistics theorem:

$$\langle \mathbf{r}_1 \dots \mathbf{r}_N | \Psi \rangle = \begin{vmatrix} \phi_a(\mathbf{r}_1) & \phi_b(\mathbf{r}_1) & \dots & \phi_n(\mathbf{r}_1) \\ \phi_a(\mathbf{r}_2) & \phi_b(\mathbf{r}_2) & \dots & \phi_n(\mathbf{r}_2) \\ \vdots & \vdots & \ddots & \vdots \\ \phi_a(\mathbf{r}_N) & \phi_b(\mathbf{r}_N) & \dots & \phi_n(\mathbf{r}_N) \end{vmatrix} \quad . \tag{3.8}$$

The choice of monoelectronic wave functions implicitly assumes the existence of an electronic mean-field[3]. Alternatively, we write the global wave function as:

$$|\Psi\rangle = \underbrace{\frac{1}{\sqrt{N!}} \sum_P (-1)^P}_{\hat{\mathcal{A}}} |\phi_a \phi_b \dots \phi_n\rangle \implies \langle \mathbf{r}_1 \dots \mathbf{r}_N | \Psi \rangle = \frac{1}{\sqrt{N}} \sum_P (-1)^P \phi_a(\mathbf{r}_1) \dots \phi_n(\mathbf{r}_N) \quad , \tag{3.9}$$

where the sum is performed over all possible permutations of the spin-orbital order and $\hat{\mathcal{A}}$ is the antisymmetrization operator. The power preceding the product of monoelectronic functions is $+1$ if the permutation is even and -1 in case it is odd[4]. The other factor normalises the state.

A variational approach is followed to obtain an estimation for the ground-state energy:

$$\frac{\langle \Psi | \hat{\mathcal{H}} | \Psi \rangle}{\langle \Psi | \Psi \rangle} \leq E_g \quad , \tag{3.10}$$

with E_g the unknown ground-state energy. Inserting expressions (3.7) and (3.9), it is possible to give an expression for $\langle \Psi | \hat{\mathcal{H}} | \Psi \rangle$ in terms of the spin-orbitals. This will be treated as a functional of the spin-orbitals to minimize the energy. The orthonormalisation condition is guaranteed including N^2 Lagrange multipliers[5] λ_{ik}:

$$\delta F = \delta \left[\langle \Psi | \hat{\mathcal{H}} | \Psi \rangle - \sum_{i,k} \left[\lambda_{ik} \left(\langle \phi_i | \phi_k \rangle - \delta_{ik} \right) \right] \right] = 0 \quad , \tag{3.11}$$

where δ_{ik} stands for the Kronecker delta. After the calculations, we arrive at the so-called

[3] This will be discussed in more depth at the beginning of Section 5.

[4] A permutation is odd if an odd number of pairs have been switched. The permutation is even if it is not odd.

[5] In practical scenarios, a unitary transformation is performed over the spin-orbitals to diagonalise the λ_{ik} matrix appearing in Eq. (3.11). Then, only N multipliers are necessary (see pp. 324-325 of [1]).

Fock equations defining of the Fock operator $\hat{\mathcal{F}}$ as in Eq. (3.13):

$$\hat{\mathcal{F}}\left|\phi_k\right\rangle = \sum_k \lambda_{jk}\left|\phi_j\right\rangle \xrightarrow{\lambda_{jk}:=\varepsilon_k\delta_{jk}} \hat{\mathcal{F}}\left|\phi_k\right\rangle = \varepsilon_k\left|\phi_k\right\rangle \tag{3.12}$$

$$\hat{\mathcal{F}} = \frac{\hat{p}_i^{\,2}}{2m_e} - \sum_i^D \frac{Z_A e^2}{4\pi\varepsilon_0 \hat{r}_i} + \sum_i^N [\hat{\mathcal{J}}_i - \hat{\mathcal{K}}_i] \quad , \tag{3.13}$$

with the direct and exchange operators respectively defined as:

$$\langle \mathbf{x}|\hat{\mathcal{J}}_i|\phi_k\rangle = \phi_k(\mathbf{x}) \int \phi_i^*(\mathbf{x}')\frac{e^2}{4\pi\varepsilon_0 r_{ik}}\phi_i(\mathbf{x}')\, d\mathbf{x}' \tag{3.14a}$$

$$\langle \mathbf{x}|\hat{\mathcal{K}}_i|\phi_k\rangle = \phi_i(\mathbf{x}) \int \phi_i^*(\mathbf{x}')\frac{e^2}{4\pi\varepsilon_0 r_{ik}}\phi_k(\mathbf{x}')\, d\mathbf{x}' \quad . \tag{3.14b}$$

It is worth highlighting the redefinition of the N^2 Lagrange multipliers λ_{ik} into N ε_k, which corresponds to the previously mentioned linear transformation of the spin-orbitals.

Note: We have kept all the constants but it is customary to use atomic units (a.u.)[6]. This would replace $e^2/4\pi\varepsilon_0 \to 1$ and $\hbar \to 1$.

The direct or Coulomb term (3.14a) describes the electrostatic interaction of an electron in ϕ_i over the electron in ϕ_k as a mean-field. The exchange operator is purely due to the antisymmetrisation of the wave function and thus describes the interaction due to the fermionic nature of electrons. The $\mathbf{x}'$ integration in Eqs. (3.14a) and (3.14b) accounts for spatial and spin coordinates.

If the Fock equations (3.12) were to be solved, one can see that the Fock operator depends on the spin-orbitals themselves, so it is necessary to start with an initial choice for those functions, solve the equations and introduce the new solution again in the $\hat{\mathcal{F}}$ definition until reaching a set threshold of convergence. This opens the question of which starting functions are optimal for the calculations. That issue will be cleared out in Section 3.3.

3.2.2 Møller-Plesset perturbation theory. Second-order corrections: MP2

The HF theory is based on a rather bold approximation for the electronic wave function. The Slater determinant captures the fermionic nature of electrons in the exchange term (3.14b) but it overlooks a fundamental feature of the system: the electronic correlation.

Electrons, as charged particles, interact by means of the electromagnetic force with each other. It is therefore unrealistic to describe the system by a single product of functions that depend only on one electron coordinates. These functions should at least consider two-body interactions as the Hamiltonian $\hat{\mathcal{H}}$ does, but the electrostatic force is captured as a mean-field term in Eq. (3.14a). It is in this wise that post-HF methods are employed in order to improve the results. In this section, we present the Møller-Plesset perturbation theory following the original formulation [2].

[6]Energies are measured in hartrees (1 Ha=27.2114 eV) and distances in Bohr radius units (a_0=0.5292 Å).

As a starting point, we will consider the difference between the actual HF energy and the sum of the $\hat{F}$ eigenvalues $\{\varepsilon_k\}$. It is proven that the following relation is fulfilled (see the note under Eq.(3.7) for the $\hat{h}_2$ definition):

$$E_{HF} = \langle\Psi|\hat{\mathcal{H}}|\Psi\rangle = \sum_k^N \varepsilon_k - \frac{1}{2}\sum_{i,j}^N \left[\left\langle \phi_i\phi_j \middle| \hat{h}_2 \middle| \phi_i\phi_j \right\rangle - \left\langle \phi_j\phi_i \middle| \hat{h}_2 \middle| \phi_i\phi_j \right\rangle \right] \quad . \tag{3.15}$$

This is the result of using the definition of $|\Psi\rangle$ in Eq. (3.9). The mean values on the right-hand side can be checked to be the ones corresponding to $\hat{\mathcal{J}}_k$ and $\hat{\mathcal{K}}_k$ in that order[7]. We can therefore state that the following eigenvalue equation is satisfied for the HF wave function:

$$\hat{\mathcal{H}}_0 |\Psi\rangle = \sum_k^N \left[\hat{\mathcal{F}}_k - \frac{1}{2}\left\langle \hat{\mathcal{J}}_k - \hat{\mathcal{K}}_k \right\rangle \right] |\Psi\rangle = E_{HF} |\Psi\rangle \quad . \tag{3.16}$$

It is now proposed to use this operator as the zeroth-order Hamiltonian for a perturbative calculation. The Møller-Plesset Hamiltonian $\hat{\mathcal{H}}_{MP}$ is thus defined as:

$$\hat{\mathcal{H}}_{MP} = \hat{\mathcal{H}}_0 + \hat{\mathcal{V}} \rightarrow \begin{cases} \hat{\mathcal{H}}_0 = \sum_k^N \left[\hat{\mathcal{F}}_k - \frac{1}{2}\left\langle \hat{\mathcal{J}}_k - \hat{\mathcal{K}}_k \right\rangle \right] \\ \hat{\mathcal{V}} = \hat{\mathcal{H}}_{MP} - \hat{\mathcal{H}}_0 = \frac{1}{2}\sum_{\substack{i,j \\ i\neq j}}^N \frac{e^2}{4\pi\varepsilon_0 \hat{r}_{ij}} - \sum_k^N (\hat{\mathcal{J}}_k - \hat{\mathcal{K}}_k) + \frac{1}{2}\sum_k^N \left\langle \hat{\mathcal{J}}_k - \hat{\mathcal{K}}_k \right\rangle \end{cases} . \tag{3.17}$$

Now, according to perturbation theory [4], the zeroth-order energy and wave function will be E_{HF} and $|\Psi\rangle$ respectively. The first-order energy correction is the mean value of the perturbation $\hat{\mathcal{V}}$ for the zeroth-order wave function.

By definition $\langle\Psi|\hat{\mathcal{H}}_{MP}|\Psi\rangle = \langle\Psi|\hat{\mathcal{H}}_0|\Psi\rangle$ so the first-order perturbation is null:

$$E_1 = \langle\Psi|\hat{\mathcal{V}}|\Psi\rangle = 0 \quad . \tag{3.18}$$

This means it is necessary to go up to at least second order to obtain a correction to the HF energy. Depending on the truncation order N, the method is named MPN. In this work, the second order or MP2 will be studied. We must highlight that the convergence is not assured for high order terms. We shall call $|\Psi\rangle = |\Psi_0\rangle$ for the rest of the calculations to indicate it is the zeroth-order wave function. In general, the second-order energy correction is given by:

$$E_2 = \sum_i \frac{\left| \langle\Psi_i| \hat{\mathcal{V}} |\Psi_0\rangle \right|^2}{E_0 - E_i} \quad , \tag{3.19}$$

[7] This result is also captured in the Slater-Condon rules [3].

where the states $|\Psi_i\rangle$ are $\hat{\mathcal{H}}_0$ eigenstates. This would mean excited states for the atomic wave function for our study. The Slater-Condon rules state that for a two-body operator such as $\hat{\mathcal{V}}$ and a wave function built as (3.9), $|\Psi_i\rangle$ and $|\Psi_0\rangle$ can differ in two spin-orbitals ϕ_i at most for the matrix elements not to be zero. Furthermore, according to Brillouin's theorem, those matrix elements involving single excited electronic functions are null[8]. This leaves us only with double excitations. We shall call $\left|\Psi_{ij}^{kl}\right\rangle$ the wave function corresponding to the excitation of the electrons in spin-orbitals ϕ_i and ϕ_j to ϕ_k and ϕ_l. The matrix elements are proven to be:

$$\left\langle \Psi_{ij}^{kl}\middle|\hat{\mathcal{V}}\middle|\Psi_0\right\rangle = \left\langle \phi_k\phi_l\middle|\hat{\mathcal{V}}\middle|\phi_i\phi_j\right\rangle - \left\langle \phi_l\phi_k\middle|\hat{\mathcal{V}}\middle|\phi_i\phi_j\right\rangle \quad , \tag{3.20}$$

so the energy correction can be obtained from the HF spin-orbitals and energies as:

$$E_2 = \frac{1}{4}\sum_{\substack{i,j\\ i\neq j}}\sum_{\substack{k,l\\ k\neq l}} \frac{\left|\left\langle \phi_k\phi_l\middle|\hat{\mathcal{V}}\middle|\phi_i\phi_j\right\rangle - \left\langle \phi_l\phi_k\middle|\hat{\mathcal{V}}\middle|\phi_i\phi_j\right\rangle\right|^2}{\varepsilon_i+\varepsilon_j-\varepsilon_l-\varepsilon_k} \quad , \tag{3.21}$$

where the sum on i, j is performed over the ground-state occupied spin-orbitals and the k, l sum over the unoccupied ones. The latter are often referred to as "virtual" spin-orbitals. The difference in (3.19) denominator is the difference of the occupied monoelectronic orbital energies in each configuration.

For a two-body operator as $\hat{V}$, these matrix elements denote the following integral:

$$\left\langle \phi_k\phi_l\middle|\hat{\mathcal{V}}\middle|\phi_i\phi_j\right\rangle = \iint \phi_k(\mathbf{x})\phi_l(\mathbf{x}')V(\mathbf{x},\mathbf{x}')\phi_i(\mathbf{x})\phi_j(\mathbf{x}')d\mathbf{x}d\mathbf{x}' \quad , \tag{3.22}$$

where $V(\mathbf{x},\mathbf{x}')$ is the result of substituting the position operators (3.17) of $\hat{\mathcal{V}}(\mathbf{x},\mathbf{x}')$ by the corresponding position vectors $\mathbf{x}$ or $\mathbf{x}'$ when projecting onto the position basis $|\mathbf{x},\mathbf{x}'\rangle$ as indicated in Eq. (3.4).

3.3 Basis sets

In order to start the self-consistent calculation, it is necessary to establish the initial guesses for the monoelectronic functions or spin-orbitals.

The monoelectronic atom is the closest system to ours whose time-independent Schrödinger equation has been solved analytically. It is customary to give these solutions as eigenfunctions of the operators $\{\hat{\mathcal{H}}, \hat{\mathcal{L}}^2, \hat{\mathcal{L}}_z, \hat{\mathcal{S}}^2, \hat{\mathcal{S}}_z\}$, which constitute a C.S.C.O. [9] for the system [5]. The orbital part of these solutions may be written as:

[8] This is only valid for the HF ground state $|\Psi_0\rangle$. Slater-Condon rules on the other hand apply to any two-body operator and functions built by means of a Slater determinant.

[9] A Complete Set of Commuting Observables is a set of quantum observables such that their common eigenvectors form a unique basis of the total Hilbert space [5].

$$\langle r \big| nlm_l \rangle = \psi_{n,l,m_l}(r,\theta,\varphi) = N e^{-\frac{r}{na_0}} \left[\sum_{q=l}^{n} C_q r^q \right] Y_l^{m_l}(\theta,\varphi) = N R_{n,l}(r) Y_l^{m_l}(\theta,\varphi) \quad . \tag{3.23}$$

The total wave function would comprise the tensor product of (3.23) and the spin eigenstate $\big|S, S_z\rangle$.

There is a big difference though with the multi-electron counterpart. The presence of many electrons involves that the potential is no longer central as it depends on the position of individual electrons. Nevertheless, the HF method approximates the electrostatic interaction as a mean field (3.14a). It could then be reasonable to consider trial functions that decay similarly to (3.23) since the field would indeed be central far from the nucleus. Each trial function would have a set of quantum numbers $\{n, l, m_l, m_s\}$ associated that stem from the assumption of a central potential.

This first class is known as STO or Slater-type orbital. They differ from (3.23) in the angular part, as the complex spherical harmonic basis is changed to real spherical harmonics, much more common in computational chemistry calculations. As an example, the set $\{Y_1^{-1}, Y_1^0, Y_1^1\}$ can be expressed in terms of real functions as it follows:

$$Y_{1,1}(\theta,\varphi) = \frac{1}{\sqrt{2}}(Y_1^{-1}(\theta,\varphi) - Y_1^1(\theta,\varphi)) = \sqrt{\frac{3}{16\pi}} \sin\theta (e^{-i\varphi} + e^{i\varphi}) = \sqrt{\frac{3}{4\pi}} \frac{x}{r} \tag{3.24a}$$

$$Y_{1,-1}(\theta,\varphi) = \frac{i}{\sqrt{2}}(Y_1^{-1}(\theta,\varphi) + Y_1^1(\theta,\varphi)) = i\sqrt{\frac{3}{16\pi}} \sin\theta (e^{-i\varphi} - e^{i\varphi}) = \sqrt{\frac{3}{4\pi}} \frac{y}{r} \tag{3.24b}$$

$$Y_{1,0}(\theta,\varphi) = Y_1^0(\theta,\varphi) = \sqrt{\frac{3}{4\pi}} \cos\theta = \sqrt{\frac{3}{4\pi}} \frac{z}{r} \quad . \tag{3.24c}$$

This comes at the cost of losing the quantum number m_l as it is no longer well-defined in these angular components. On the other hand, STOs may be defined in two representations: cartesian or spherical. These are respectively defined as:

$$\psi_{STO}(r,\theta,\varphi;\ l,m;\ \xi) = K r^l e^{-\xi r} Y_{lm}(\theta,\varphi); \qquad \psi_{STO}(x,y,z;\ a,b,c;\ \xi) = K x^a y^b z^c e^{-\xi r} \quad , \tag{3.25}$$

with K a normalisation constant. Nevertheless, this study will not make use of STOs but of their gaussian version GTOs:

$$\psi_{GTO}(x,y,z;a,b,c;\xi) = K x^a y^b z^c e^{-\xi r^2}; \qquad K = \left(\frac{2\xi}{\pi}\right)^{3/4} \left(\frac{8\xi^{(a+b+c)} a!b!c!}{(2a)!(2b)!(2c)!}\right)^{1/2} \quad . \tag{3.26}$$

They can also be defined in spherical form similarly to STOs. The reason behind this change is the computational advantage of using Gaussian functions to calculate double-orbital integrals, such as (3.15). There is no analytical solution for those integrals for STOs trial functions. The sum of exponents $a + b + c = l$ is the total orbital momentum of the monoelectronic orbital. These functions are plotted below to give a spatial sense to them,

which is one of the reasons why the original basis was changed[10]. The following scatter plots in Figure 1 show the spatial distribution for $a + b + c = \{0, 1, 2\}$ evaluated for a random ensemble of points in the $[-2, 2] \otimes [-2, 2] \otimes [-2, 2] \in \mathbb{R}^3$ domain for $K = \xi = 1$.

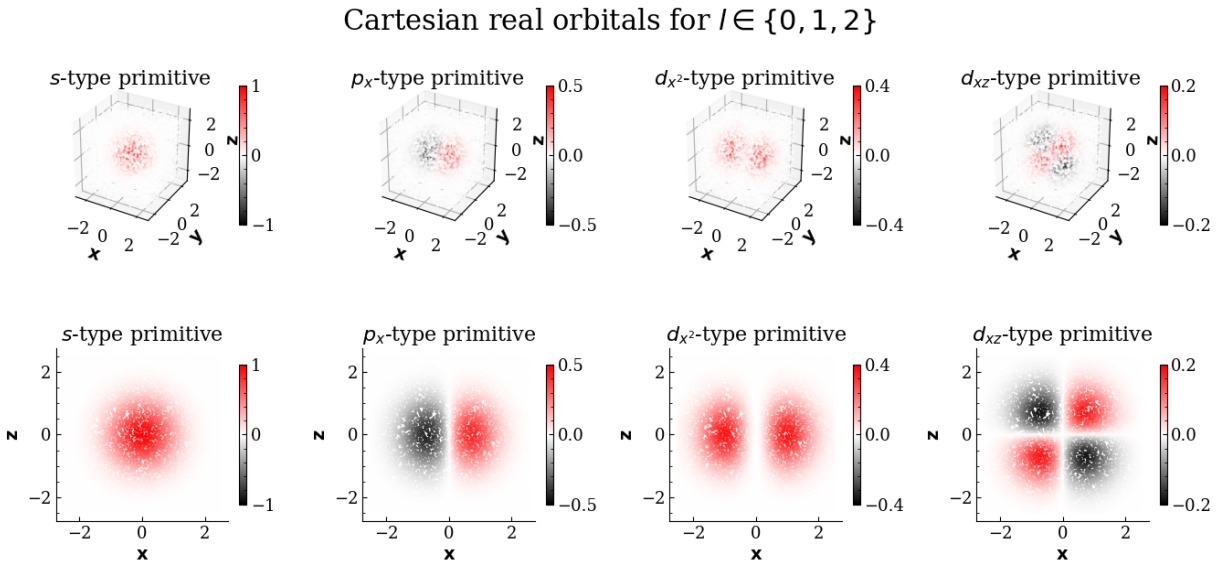

Figure 1: Spatial distribution of cartesian GTOs with $a + b + c = \{0, 1, 2\}$. In this order from left to right, the parameters (a,b,c) of (3.26) were set to (0,0,0), (1,0,0), (2,0,0) and (1,0,1). The plots in the second row show the cut of the GTOs with the plane y=0. Figure produced by the author.

There are several problems still if these were the trial monoelectronic functions for a HF calculation. First of all, we must consider the fact that the H atom analytical solution decays as an STO, not as a GTO. Secondly, from the knowledge we have of this atom in particular, the eigenfunctions of the foregoing C.S.C.O. take more exotic shapes than a mere gaussian. Thirdly, considering these calculations are mainly performed over molecules that may have hundreds of electrons with their corresponding molecular orbitals both occupied and virtual, the search of the minimizing exponents ξ should be performed as efficiently as possible.

For this reason, GTOs are not used on their own but rather a linear combination of them. Each one of these linear combinations is called primitive. A primitive has a well-defined angular momentum l so $a + b + c$ is constant for a contraction. A set of primitives is called a basis set. To cover the third problem, each atom has several predetermined basis sets where the contracting coefficients have already been determined based on previous results for different molecules and atoms. This constitutes an important step because it sets an initial guess for the calculation through a linear combination of atomic orbitals (LCAO) that are already tabulated.

As the specific orbital shape for a given system is conditioned by the atomic neighbourhood, the HF method optimizes a second set of coefficients that combine the primitives of the system under study.

There are no restrictions on how to build a basis set and its primitives. Therefore, basis

[10]This should come without surprise as important structural information of a given molecule can be extracted from the charge density. Retrieving this information from a complex-valued function would certainly be a more difficult task.

sets are gathered in families according to their structure, some of which will be briefly discussed.

Minimal basis sets. STO-NG A minimal basis set only has one primitive per occupied orbital. Therefore, for the C atom for instance, 3 primitives ($1s$, $2s$ and $2p$) are defined. A common family of minimal basis sets is the STO-NG [6], named this way because they intend to reproduce an STO orbital with the linear combination of N GTOs:

$$\psi_{STO*}^{n,l} = \sum_{i}^{N} d_i \psi_{GTO}(x, y, z;\ l;\ \xi_i) \quad . \tag{3.27}$$

In order to accelerate the convergence, the exponents ξ_i of $\psi_{STO*}^{n,l}$ associated with the same principal quantum number n are kept equal. The star "$*$" means that the contraction is an approximation to a true STO. The coefficients d_i and ξ_i were determined by minimizing the difference between a given STO, which were more common before the development of this basis sets, and the linear combination of GTOs.

Finally, the HF method is implemented by means of the Roothaan equations:

$$\hat{F}C = SC\varepsilon \quad , \tag{3.28}$$

which are none other than the Fock equations (3.12) in matrix form. $\hat{F}$ is the Fock operator, C is a coefficient matrix that will be minimized by the HF method and ε is the diagonal matrix of the Fock eigenvalues ε_k. S is the overlap matrix composed by terms $S_{ij} \left\langle \phi_i \middle| \phi_j \right\rangle$ as the primitives are not orthonormal generally speaking. In this hypothetical case, S would be the identity. To conclude, Eq. (3.28) constitutes the altered version of the Fock equations to include the basis set formalism.

The final monoelectronic wave functions are then the linear combination of the primitives according to the coefficient matrix C when the HF converges.

Split-valence basis sets. Pople bases The split-valence basis sets are the natural continuation of the STO-NG but allowing for more flexibility. They were developed by the research group of J. A. Pople [7] [8]. The split-valence basis sets make a distinction between core and valence electrons, giving more flexibility to the latter by allowing multiple primitives per orbital. These sets are noted as X-IJKg. X is the number of contracted GTOs for the core primitives, while the numbers after the hyphen convey the number of contracted GTOs for each valence orbital primitive. For instance, a 4-31g set for the C atom means a contraction of 4 GTOs for the $1s$-orbitals and two primitives for the $2s$ and $2p$-orbitals, the first consisting of a 3-GTO contraction and the second of a single GTO. for a total of 5 primitives. We can note this as (8s,4p)→[3s,2p], that is, the contraction of 8 s-GTOs and 4 p-GTOs in 3 s-primitives and 2 p-primitives.

The exponents ξ_i are also shared for subshells of equal n, and the parameters are minimized in terms of the total atomic energy[11].

[11] This work studies atomic systems, so the parameters are, in fact, the best possible set. This is not true for molecular applications but constitutes a good starting point.

It is usual to see these sets augmented with some type of additional GTOs. Doubled symbols always refer to H atoms.

- If a "*" is present as in 6-311g*, an extra set of higher angular momentum functions are included to improve the accuracy of the correlation energy at the MP2 stage. Two "**" include 1 p-GTO for H atoms.
- If the set has a "+" as in 6-311+g one diffuse i. e. with a low exponent ξ, a sp-GTO[12], is added to the set of primitives. Two "++" involve the addition of a diffuse s-GTO for the H atom.

The determination of these functions is made by "using well established *rules of thumb* or by explicit optimization" [9].

Correlation consistent basis sets. Dunning bases Correlation consistent basis sets were developed by Thom. H. Dunning Jr. [9] by optimization of configuration interaction (CI) calculations for atoms. They always have higher angular momentum GTOs to improve the correlation calculations in their initial formulation. Again, they can include two functions per valence orbital (cc-pvdz), three (cc-pvtz), four (cc-pvqz) and so on. The addition of diffuse functions is labelled with the prefix "aug" as in (aug-cc-pvdz). Their name (correlation consistent) note that the contracted primitives of a given angular momentum are built from the same set of GTOs instead of defining one set per contraction as in STO-NG or split-valence basis sets.

Polarization consistent basis sets. Jensen bases These sets were developed by Frank Jensen [10] to adapt correlation consistent basis sets, which were thought for post-HF methods, to DFT calculations. While this project is not focused on this formulation, they constitute a more complex and larger basis set that was found useful for the electron affinity calculation. The notation is pc-n, with n the difference between the highest angular-momentum GTO in the basis and the highest angular-momentum atomic ground-state orbital. For Ne, for instance, pc-1 contains one d-GTO, pc-2 contains one f-GTO, etc. The augmented diffuse expansion uses again the prefix aug-pc-n.

The notation we will use to identify calculations will be "**method(basis)**" as in **HF(6-311g*)**. All the bases used were in cartesian representation.

4 NWChem

En esta sección se presenta NWChem, el programa empleado para los cálculos computacionales y se describe la estructura del fichero de entrada básico para los cálculos HF y MP2.

NWCHEM is a free distribution computational ab initio chemistry package developed by the Experimental Molecular Science Laboratory (EMSL) at the Pacific Northwest National

[12]The importance of diffuse functions in the reproduction of low bounded electrons is described in Section 5.3

Laboratory (PNNL) [11]. It allows for quantum mechanical calculations ranging from HF and post-HF methods to DFT, both relativistic and non-relativistic as well as quantum and classical molecular dynamics. The package was developed to perform molecular calculations in the context of biomolecules or nanostructures, but we have adapted it to the atomic domain. All calculations in this work were run in node 41 of the cluster Molec3 in the Department of Physics of the University of La Laguna. In order to start the calculations, the user must provide the program with an input file where the system is defined and constraints are settled. We devote the following section to detail its structure.

4.1 Input file structure

NWCHEM retrieves the specifications for the desired calculations from an input file. This file is divided into directives, each of which is devoted to a specific aspect of the calculation. Some examples of these are:

- ECHO. Prints the input file at the beginning of the output file. It is not needed for the calculations but advisable to identify the file.
- START. It will name all the files associated with that calculation as the word written next to the directive plus their extensions. It not mandatory.
- TITLE. The title for the output file.
- GEOMETRY. Specifies the geometry of the system. Each atom must be identified with its symbol and the (x, y, z) coordinates where the nucleus will be fixed.
- BASIS. Must be specified whether the cartesian or spherical projection is used. If the calculation involves different classes of orbitals, the type must be specified. Default is "ao basis" (atomic orbital). A basis must be chosen for each atom specified in the GEOMETRY directive. The available bases for each atom can be checked in [12].
- PRINT. Controls the level of detail offered by the output file. It is often unnecessary but sometimes a greater level of depth could be desired. For instance, the details for the inner level of atoms are not displayed unless the "debug" level is selected.
- TASK. It specifies the type of calculation to be performed. Both the method and aim of the calculation must be specified. The ones that will be employed in this work are the "SCF energy"[13] and the "MP2 energy"[14]. The first word sets the method to obtain the result specified by the second, "energy" in this case. Other possibilities are the minimization of the atomic positions in the context of molecular calculations with "optimize" or the normal modes with "frequencies". Coupled cluster (CC) calculations are also available for closed-shell systems.
- SCF/MP2/DFT... These are directives related to the chosen method. They must be specified before the TASK directive. The subdirectives depend on the method. As this work is focused on the HF and MP2 method, we will mention the most important ones for the HF method:

[13] Stands for "self-consistent field".

[14] A brief mention about the density functional theory (DFT) will be made in the conclusions.

  - MAXITER. Sets the maximum number of iterations. Default is 30.
  - RHF/ROHF/UHF. Restricted Hartree-Fock, restricted open-shell Hartree-Fock and unrestricted Hartree-Fock respectively. The first one constrains the configuration to orbitals filled with paired electrons, the second does the same for the core electrons, keeping free orbitals for unpaired electrons; and the third calculates / ↑ and ↓ orbitals[15] separately. RHF is the default option.

    The MP2 calculation is only available for RHF and UHF.
  - DOUBLET/TRIPLET/QUARTET... Sets the spin multiplicity ($2S + 1$) of the system. This is a mandatory constraint for ROHF and UHF calculations. The occupation of orbitals for the ground state will always satisfy this spin multiplicity. SINGLET is the default option.
  - THRESH Sets the threshold for the convergence of the energy calculation. The default is 10^{-6} for the HF method and 10^{-8} for the MP2 in atomic units.

- SET TOLGUESS X. X is the accuracy threshold in Ha for the initial guess for the atomic orbitals. Default is 1e-7 Ha. This guess may be of great importance as the occupation numbers are assigned at this stage.

Additional information on the program and its capabilities can be found in the Users Manual posted on GitHub [13].

5 Results and discussion

En esta sección se presentan los resultados principales obtenidos con NWChem. Se realiza un estudio de los niveles monoelectrónicos ocupados para los átomos H-Kr así como predicciones de las energías de ionización y afinidades electrónicas para justificar la exactitud del método. También se discute la importancia de las funciones difusas en la simulación de sistemas con electrones débilmente ligados.

First of all, we must discuss a couple of well-known results in the study of atomic physics. The notion of *orbital* stems from the solutions of the time-independent Schrödinger equation. These accessible states for the electron allow introducing the somewhat misleading idea of the electron occupying a predetermined orbital, when in fact, the probability distribution of the electron is just a consequence of the system's Hamiltonian (3.5), that is, there are no prefixed orbitals where the electrons are located.

This conception could be used without much problem in a hydrogen-like atom, where only one electron is interacting with the nucleus. Nevertheless, when we are dealing with a trial wave function as the one in Eq. (3.9), this notion of an electron occupying a single spin-orbital is proven false. The projection of this wave function in the position basis in Eq. (3.9) shows that electrons are simultaneously "occupying" all the spin-orbitals. Therefore, this notion of a monoelectronic level is not correct from the very beginning.

[15]The notation α and β electrons is also common instead of ↑ and ↓

An attempt to conciliate this idea and to solve the multi-electron problem is the mean-field approximation. This approximation takes the electronic repulsion and roughly approximates it as a central potential, which is in general not the Coulomb potential, as it depends on the mean electronic distribution[16]. The difference between the actual potential and the mean-field approximation could then be included as a small perturbation. In this regard, we would find orbitals "ready to allocate" each electron just as in a hydrogen-like atom, each with its well-defined quantum numbers $\{n, l, m_l, m_s\}$. These are not true but just an approximation given the fact that the potential is not actually central[17].

There are two important results concerning the mean-field approximation. The first of them is the Aufbau principle:

Aufbau principle

For the ground state of an atom or ion the electrons will fill the lowest energy levels, without violating Pauli's exclusion principle.

Secondly, the filling order will take place in a specific order according to the electron quantum numbers:

The n + l rule

The electronic orbitals will be filled in increasing order of $n + l$. If there is more than one possible set of orbitals, the electron will occupy the orbitals with the highest l.

The name of this filling rule is rather unclear and attributed to several authors. Therefore, we will refer to it as the "$n + l$ rule"[18].

Combining these two rules, it is possible to build a filling sequence to predict the order in which the monoelectronic orbitals will be filled:

$$1s\ 2s\ 2p\ 3s\ 3p\ (4s\ 3d)\ 4p\ (5s\ 4d)\ 5p...$$

The order of terms between parenthesis depends on the central potential that is considered. We shall prove this result is partially correct in the following discussion as it describes very accurately light atoms but fails to capture the complexity that some species present in their electronic configuration.

Lastly, given one electronic configuration, the $n + l$ rule does not provide any information on whether there is a preference for a certain m_s quantum number[19]. In this context, we introduce the first Hund's rule:

[16] This idea is somehow captured in the Coulomb term (3.14a) in the HF theory.

[17] Except for closed-shell systems. This will be demonstrated in the diagrams for energy levels in Figures 2, 7, 8 and 12.

[18] Other usual denominations are Madelung's rule or the diagonal rule.

[19] The m_l quantum number is lost when the real orbitals are built from the original basis as shown in Eqs. (3.24a-c)

Hund's maximum multiplicity rule

Given an electronic configuration, the electrons will occupy the orbitals that allow the maximum spin projection $M_S = \sum_i^N m_{s_i}$.

This means that there will be a tendency for electrons to be located with their spin parallel to one another. This spin interaction is captured in the exchange term (3.14b) in the HF theory

5.1 HF calculations for light atoms

5.1.1 HF ground-state energies

The ground-state energies for each atom with $Z \in [1, 10]$ were calculated using a HF method. Different spin multiplicities[20] have been tested in order to check their effect on the results. The lower the energy, the more stable the configuration will be and it will thus be preferred by the system.

Table 1: ground-state energies in Ha for atoms and their respective first positive ions for $Z \in [1, 10]$ with spin multiplicity constraint for a HF(6-311g*) calculation. The lowest-energy configuration will be considered the ground state. Those energies are highlighted in **bold**. Calculations that failed to converge are marked with "**?**".

	Neutral atoms						Positive ions				
	Singlet	Doublet	Triplet	Quartet	Quintet		Singlet	Doublet	Triplet	Quartet	Quintet
H	-	**-0.4998**	-	-	-	**H^+**	-	-	-	-	-
He	**-2.8599**	-	**?**	-	-	**He^+**	-	**-1.9981**	-	-	-
Li	-	**-7.4321**	-	**?**	-	**Li^+**	**-7.2358**	-	**?**	-	-
Be	**-14.5719**	-	-14.5120	-	**?**	**Be^+**	-	**-14.2764**	-	**?**	-
B	-	**-24.5302**	-	-24.4499	-	**B^+**	**-24.2353**	-	-24.1197	-	**?**
C	-37.5988	-	**-37.6892**	-	-37.5951	**C^+**	-	**-37.2920**	-	-37.1583	-
N	-	-54.2589	-	**-54.3981**	-	**N^+**	-53.7611	-	**-53.8863**	-	-53.7396
O	-74.6780	-	**-74.8053**	-	-73.9375	**O^+**	-	-74.1801	-	**-74.3648**	-
F	-	**-99.3969**	-		-	**F^+**	-98.6595	-	**-98.8206**	-	-97.5414
Ne	**-128.5227**	-	-127.0425	-	-125.54321	**Ne^+**	-	**-127.7968**	-	-126.1722	-

This is not the true ground-state energy since the HF is variational based, but the lowest energy for each chemical species shall be considered the true ground-state electron configuration. According to their number of electrons, it is possible to pose triplet and quartet states for He and Li respectively, but the HF calculation yields an error and fails to converge. The differences in energy between those configurations and the ones appearing in Table 1 are so high that the initial guess is not enough to attain the convergence. Nevertheless, the basis set 6-31g* does provide values for both. For instance, the He singlet has an energy of -2.855 Ha while the triplet is a less bounded configuration with -1.399 Ha.

Analytical and exact results for H and He^+ yield 0.5 Ha and 2 Ha. Results in Table 1 show the degree of accuracy of the method. It can be seen that the approximation is reasonably

[20]The spin multiplicity is defined as g=(2S+1) with S the total spin angular momentum of the system. A state with g=1 is named a singlet, g=2 a doublet, etc.

accurate. The comparison with experimental data will always entail the energy difference of two computational states. As a result, we expect that these minor differences will cancel out for similar systems to provide good predictions.

It is also possible to retrieve data concerning each monoelectronic orbital, both occupied and virtual. The energy diagrams in Figure 2 indicate the spin projection m_s, angular momentum l and energy for all the occupied spin-orbitals as well as for the lowest energy virtual ones. It resembles the typical molecular orbital diagrams but adapted to the atomic system.

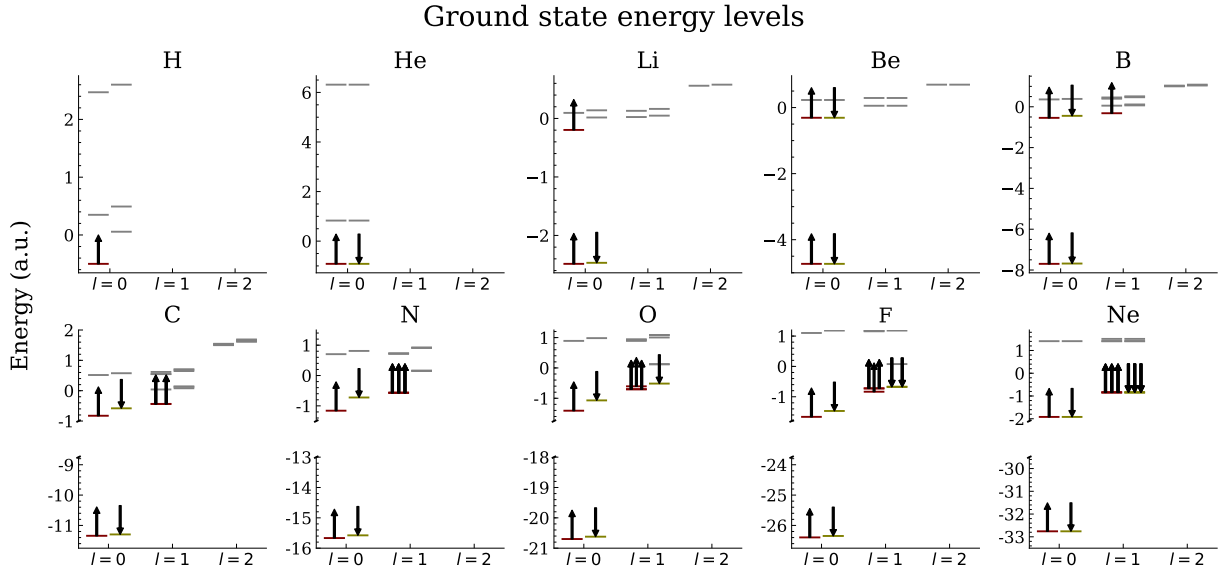

Figure 2: orbital filling for the ground states of atoms with $Z \in [1, 10]$ according to a HF(6-311g*) calculation. The monoelectronic orbitals are sorted into 3 columns according to their angular momentum $l \in \{0, 1, 2\}$. Each group is then divided in two, ↑ on the left and ↓ on the right to analyse the effect of the spin in the energetic structure. The filled orbitals (E<0) are marked with an arrow that also indicates the spin projection. The orbitals marked in grey are unoccupied or virtual (E>0).

First of all, Figure 2 shows the occupied orbitals resulting from the convergence of Fock's equation (3.12). The electronic configuration for an atom with atomic number Z approximately preserves the energetic structure and electronic distribution of atoms with $Z' < Z$. In other words, the presence of one extra electron does not have a huge impact on the preceding level structure but it is added to the following level energetically speaking. Figure 2 justifies the Aufbau principle for these atoms.

Secondly, a more detailed analysis confirms that the $n + l$ rule holds for these light atoms. Even though NWChem does not provide the principal quantum number n, Figure 2 shows the filling of a first s-orbital for H and He, a second s-orbital for Li and Be and finally 3 p-orbitals for B through Ne. These three groups may be identified with the $1s$, $2s$ and $2p$ orbitals stemming from the mean-field theory. This analogy asserts the validity of the central field approximation.

Thirdly, we notice that the filling of the, at least in theory, 3 degenerate $2p$ orbitals follows a characteristic pattern. After the filling of one p-orbital for the B atom, a second electron with equal m_s occupies a second $2p$ orbital for C, followed by a third for a triple degenerate level in N. At this point, and if we follow the $n + l$ rule, Pauli's exclusion principle forces the next electron to have opposite projection. This breaks the degeneracy of the N atom

electron triad and one of them is slightly more energetic than the remaining two. The addition of a second ↓ electron shifts the degeneration of the three ↑ and two of them are placed on a slightly more energetic orbital. Finally, Ne completes the subshell.

This discussion lacks some physical sense as it is formulated in the context of the central field approximation. All the electrons belong to all the orbitals at the same time, but these remarks help to justify and discuss the validity of the main hypothesis and results of the model. Remarkably, the assumption of a central field involves n and l-dependent energy levels, but Figure 2 shows a dependence on the spin projection m_s. This is an effect is due to the exchange term $\hat{\mathcal{K}}$ (3.14b). This allows justifying Hund's rule of the maximum multiplicity in terms of the orbital energy. As the orbitals are consistently lower in energy than the ↓, there will be a preference to occupy the first, systematically increasing the multiplicity of the system until Pauli's exclusion principle forces the electrons to have a $m_s = -1/2$ projection. This dependence on the spin disappears when the atom has a closed subshell as in He, Be and Ne. In this case, the orbital energy is n and l dependent, recovering the structure due to a true central potential.

Lastly, the diagram allows us to see two different energy bands where the electrons are placed; the $1s$ orbital is far more bounded in comparison to the $2s$ and the $2p$ orbitals. From a purely electrostatic point of view, this effect must mean that either those orbitals entail a higher presence probability further from the nucleus or that the effective charge of the latter is smaller. In this last scenario, the lower energy electrons must also be closer to the nucleus in order to screen some of its charge. An angular integration of the occupied orbitals yields a radial density plot for each of the atoms previously discussed. The radial density is defined as:

$$\rho(r) = \int_\Omega r^2 |\Psi(r,\theta,\varphi)|^2 d\Omega = \sum_i^N \int_\Omega r^2 |\phi_i(r,\theta,\varphi)|^2 d\Omega \tag{5.1}$$

where Ω refers to the solid angle and ϕ_i to an occupied spin-orbital.

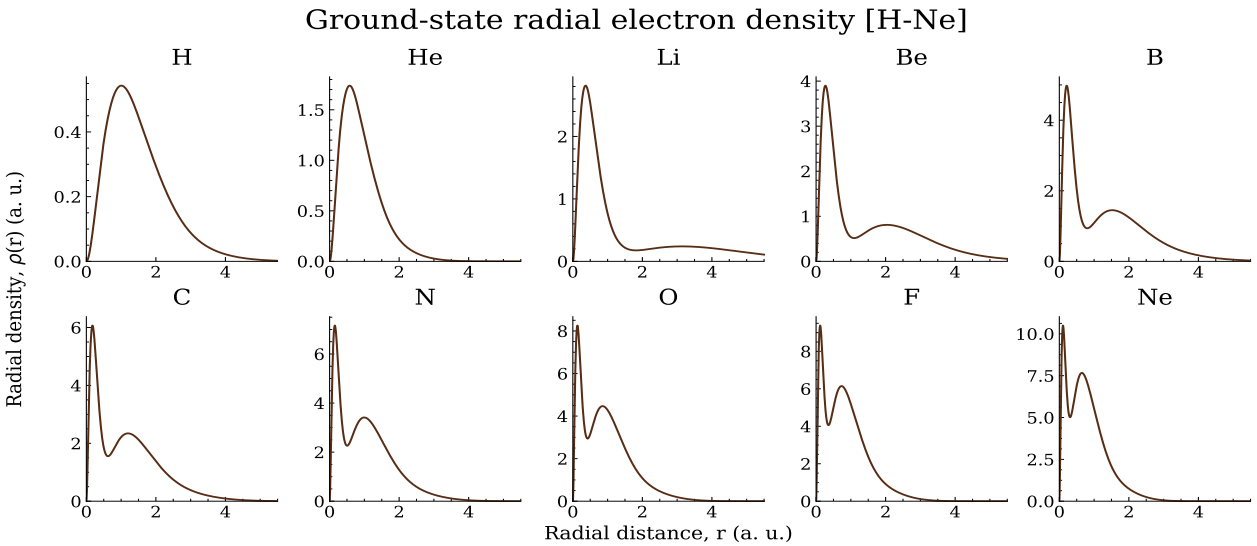

Figure 3: radial electron density for the neutral atoms with $Z \in [1, 10]$. The area under the curves corresponds to the number of electrons N of the system. The scale has been adjusted to easily compare the plots for different elements.

Figure 3 shows the progression of the radial electronic density when Z increases. The plots confirm that the energy gaps can be partly explained due to the radial distance that separates the electrons from the nucleus[21]. In addition, the displacement of the density peaks in Figure 3 shows the effect of the increasing nuclear charge on the electrons. This tendency is better seen in the following graphic:

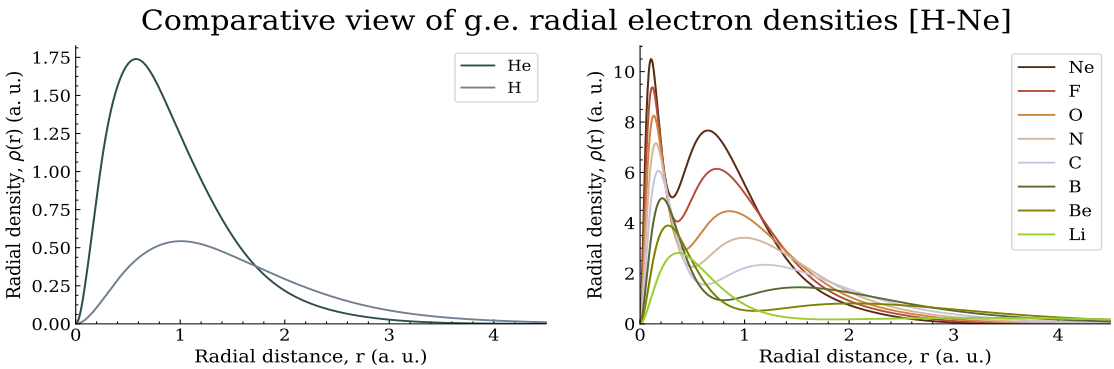

Figure 4: superimposed radial electron density plots of Figure 3 for the ground state of neutral atoms with $Z \in [1, 10]$. 1^{st} and 2^{nd} period atoms have been plotted in different graphs.

The plot on the right shows how even though the only difference in the electronic structure of Ne and F is an extra electron in an orbital $2p$, with low presence probability when $r \to 0$ (p orbital), this extra particle affects the density near the nucleus. This happens because the extra electron is located in all the orbitals simultaneously.

5.1.2 Ionization energies

Up to this point, all the discussion has been centered around the understanding of the theoretical electronic arrangement. However, the atomic energies contained in Table 1 lack any physical meaning since the 0 is arbitrarily set at the energy in which the atoms would dissociate[22]. In order to connect this study to the experimental data, the ionization energies of these atoms are compared to the expected values according to the results in Table 1. The difference between the ionic and atomic ground-state energies account for the minimum energy supply needed to extract one electron from the atom.

$$\mathrm{X} + \text{energy} \longrightarrow \mathrm{X}^{+} + e^{-} \quad . \tag{5.2}$$

Results for both the HF(6-311g*) and HF(STO-3G) basis sets are shown in Figure 5 to visualise the impact of the basis set choice.

This magnitude is also compared with the highest energy for an occupied monoelectronic orbital of the atomic configurations. Koopmans' theorem [14] for closed-shell systems states that the energy of the last occupied orbital can be regarded as a good approximation for the first ionization energy.

The values obtained by the STO-3G basis are generally worse than the ones that the split-valence basis 6-311g* yields. The absolute error, which is due to the electronic correlation

[21] The angular momentum of the monoelectronic orbital is also a factor to take into account.
[22] This means a situation in which all particles (nucleus and electrons) are separated at an infinite distance.

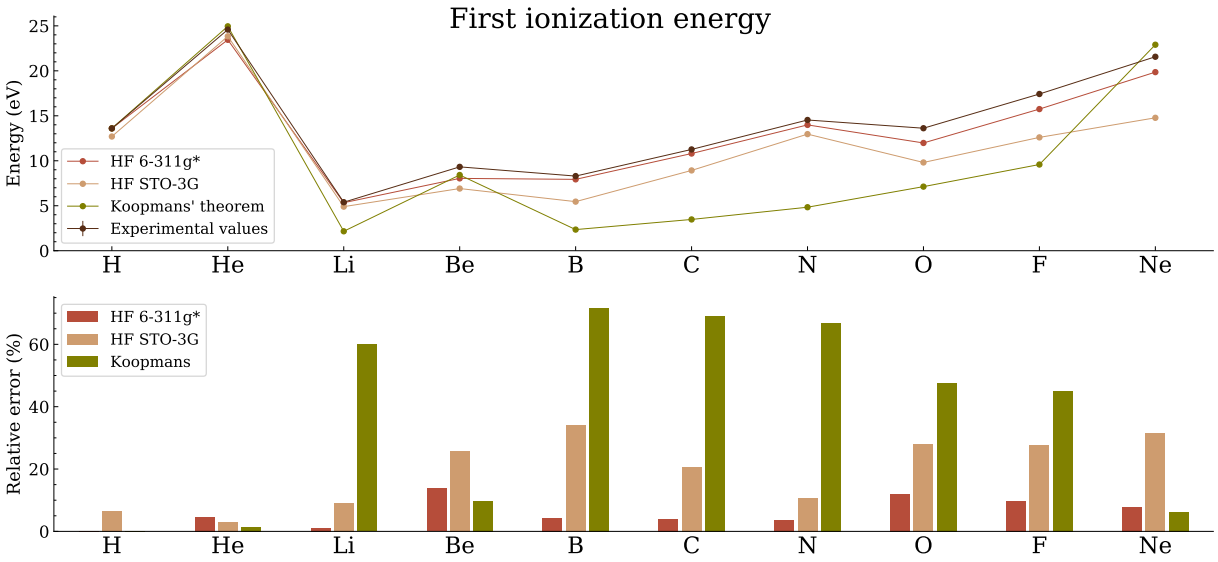

Figure 5: First ionization energy for atoms with $Z \in [1, 10]$ according to HF calculations for the basis sets 6-311g* and STO-3G as well as the prediction drawn by Koopmans' theorem. The lower graph shows the relative error between the three methods and the experimental values [15].

energy and relativistic and hyperfine corrections, lies within a 2 eV gap according to the NIST database [15], from where the reference data have been retrieved.

Koopmans' theorem becomes quite accurate for closed-shell systems (He, Be and Ne) but fails to predict accurately the rest of the ionization energies. This result is commonly used for molecular applications given the closed-shell nature of the majority of molecules.

According to the experimental values, closed-subshell atoms as well as the N, whose electrons fill half of the valence p orbital, show higher stability than their respective neighbours in terms of the atomic number Z. This behaviour is replicated in both of the HF calculations. One could wonder about how accurately this magnitude may be predicted. This is discussed in the next section, where an MP2 calculation is performed over the HF solutions.

5.2 Extension to heavier atoms. MP2 refinement

After the introduction developed in the previous section for light atoms, a similar procedure is followed for the subsequent atoms in the periodic table up until Z=36 or krypton atom (Kr).

It is assumed that the $n + l$ rule is fulfilled in order to obtain the ground state. A HF(6-311g*) and MP2(6-311g*) calculations are carried out to estimate the electronic correlation energy and obtain better results for the ionization energies.

Figure 6 contains the ionization energies for the ground state of atoms ranging from H to Kr, excepting the so-called transition metals (Sc-Zn). Those are discussed afterwards in a separate section. The exact numeric values for atomic and ionic ground states can be checked in Appendix B, Table 9.

The HF electronic configurations that led to the previous results for the neutral atoms are

shown in Figures 7 and 8.

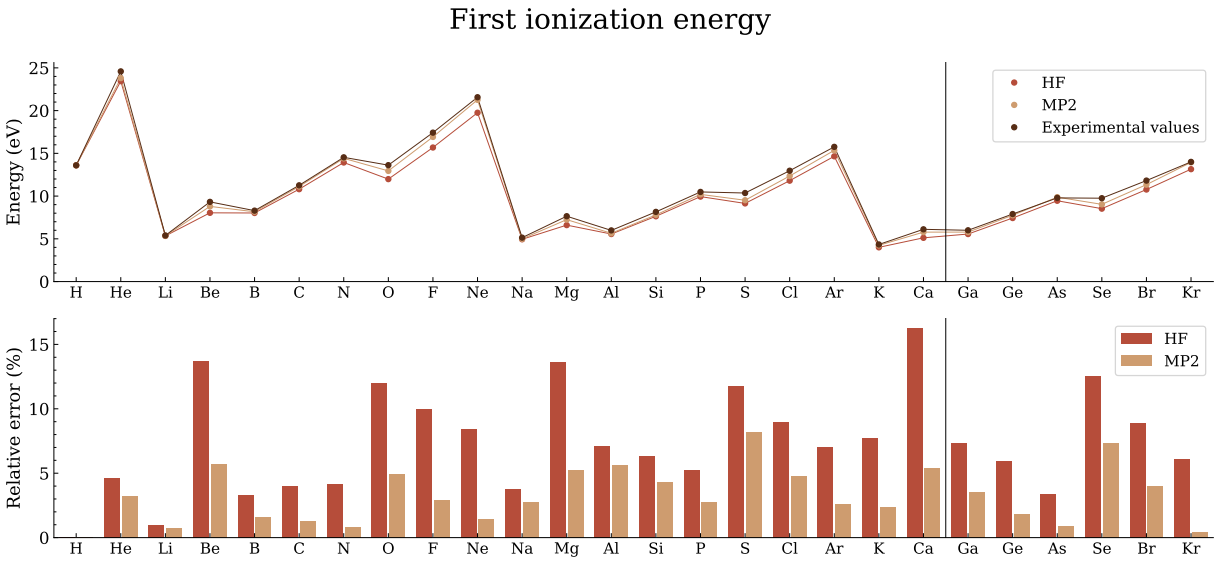

Figure 6: First ionization energy for atoms with $Z \in [1, 20]U[30, 36]$ according to HF(6-311g*) and MP2(6-311g*) calculations. The lower graph displays the relative error between both predictions and the reference values [15]. A vertical black line marks where the transition elements would be located.

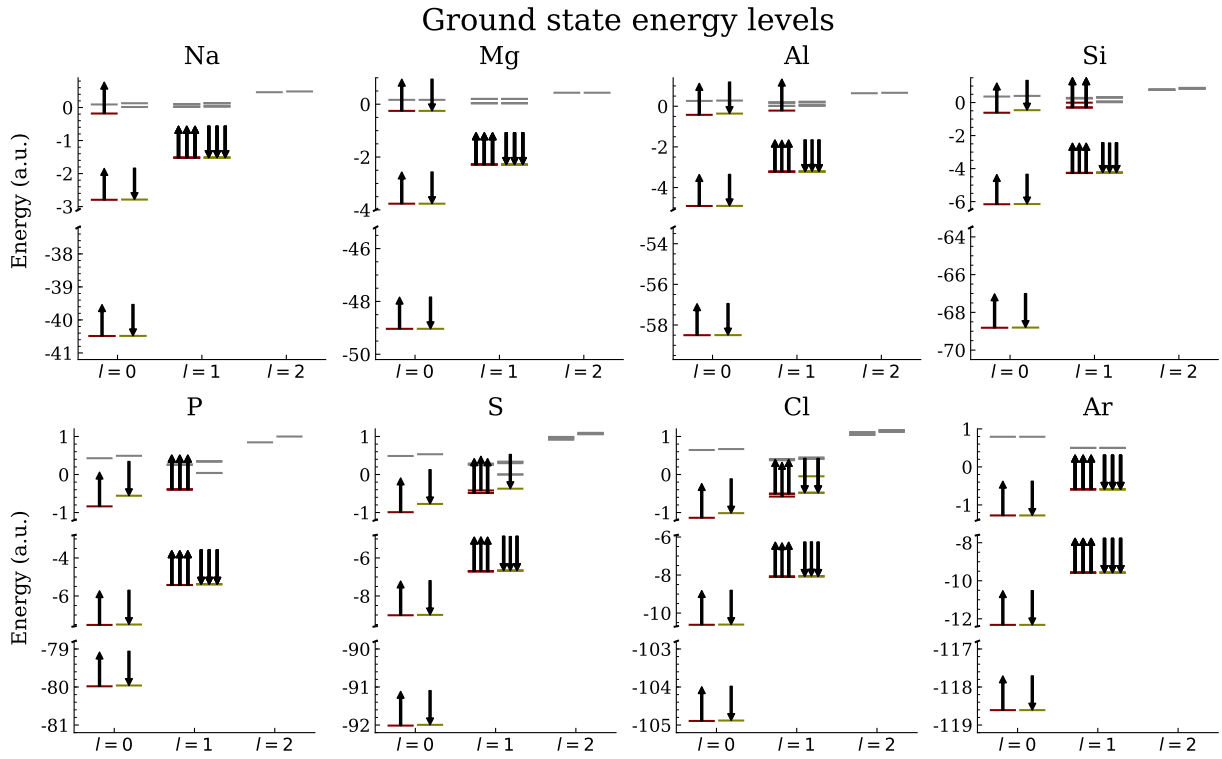

Figure 7: orbital filling for the ground states of atoms with $Z \in [11, 18]$. The monoelectronic orbitals are sorted into 3 columns according to their angular momentum $l \in \{0, 1, 2\}$. The filled orbitals are marked with an arrow that also indicates the spin projection. The orbitals marked in grey are unbounded (E>0).

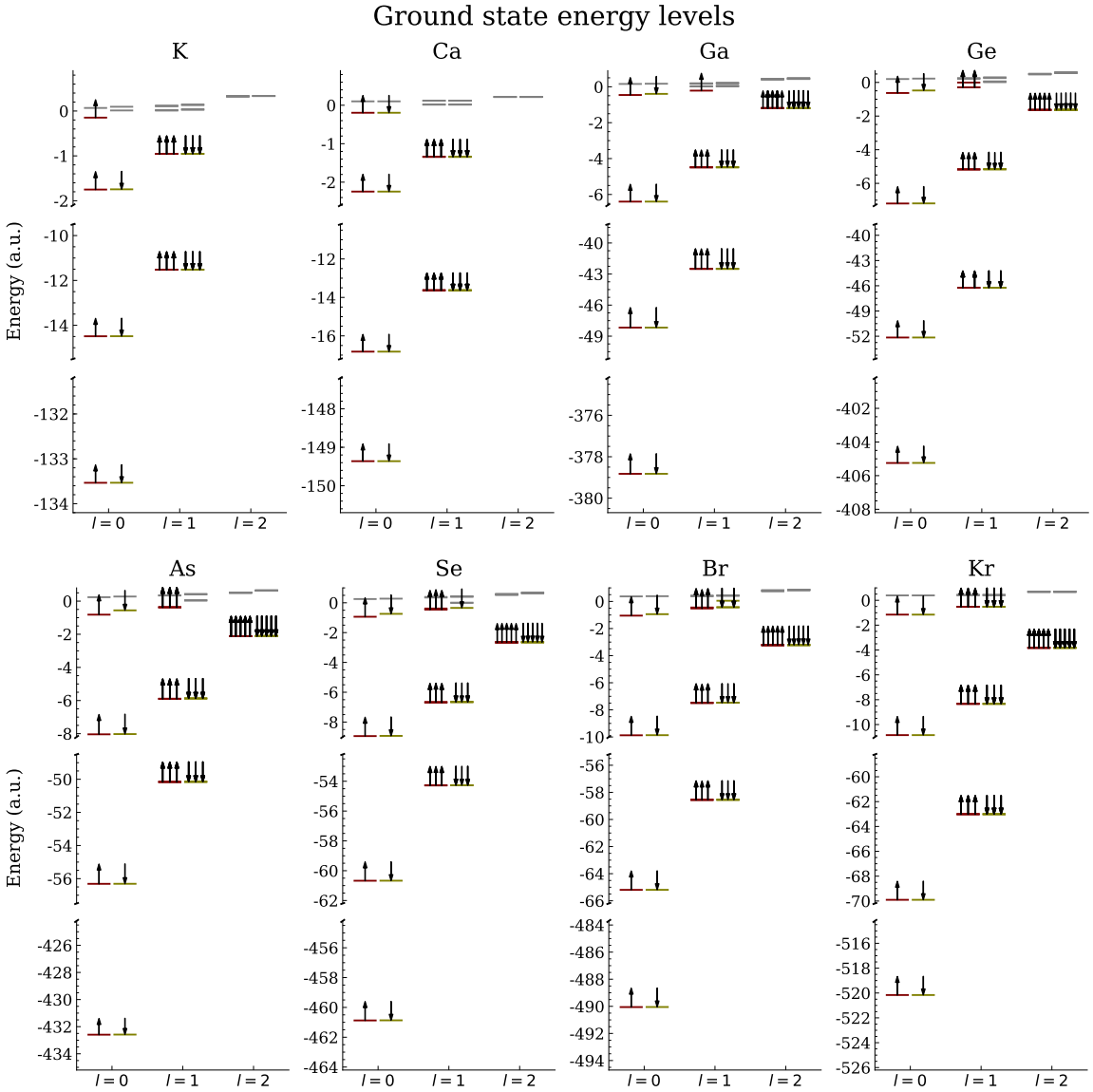

Figure 8: orbital filling for the ground states of atoms K-Ca and Ga-Kr according to a HF(6-311g*)$_c$ calculation. The monoelectronic orbitals are sorted into 3 columns according to their angular momentum $l \in \{0, 1, 2\}$. The orbitals marked in grey are unoccupied or virtual (E>0).

The MP2 calculation always improves the predicted values for the ionization energies. The expected periodicity of the results is reproduced, and some conclusions may be drawn at this point when comparing the energy level diagrams and the reproduced ionization energies:

- The highest ionization energies correspond to atoms with a filled valence subshell with *p* orbitals (He, Ne, Ar, Kr).
- The slight crest found for the 15^{th}-group elements (N, P and As) correspond to atoms whose electronic structure features a half-filled valence subshell with *p* type orbitals.
- The MP2 calculation allows reducing the absolute error within a 1 eV margin.

- Both the Hartree-Fock and the MP2 calculations consistently underestimate the ionization energy (excepting the As atom, where the MP2 yields a slightly higher energy).
- Interestingly, the highest values for the ionization energies (15^{th} and 18^{th} group) are among the best predictions regarding the relative error even though their experimental values are higher in comparison to nearby groups.

This first diagram shows an electronic configuration quite similar to the previous in Figure 2. It can be seen that the electronic configuration showed in that diagram is maintained in Figure 7 and the same order is followed as the filling continues, that is, the electrons are arranged with the maximum spin multiplicity within the same subshell and ↑ levels are more bounded than ↓. As there is a big energy gap between the $2p$ and $3s$ subshells, we expect that the electron density displays a third peak as the 3s and 3p subshells are being completed.

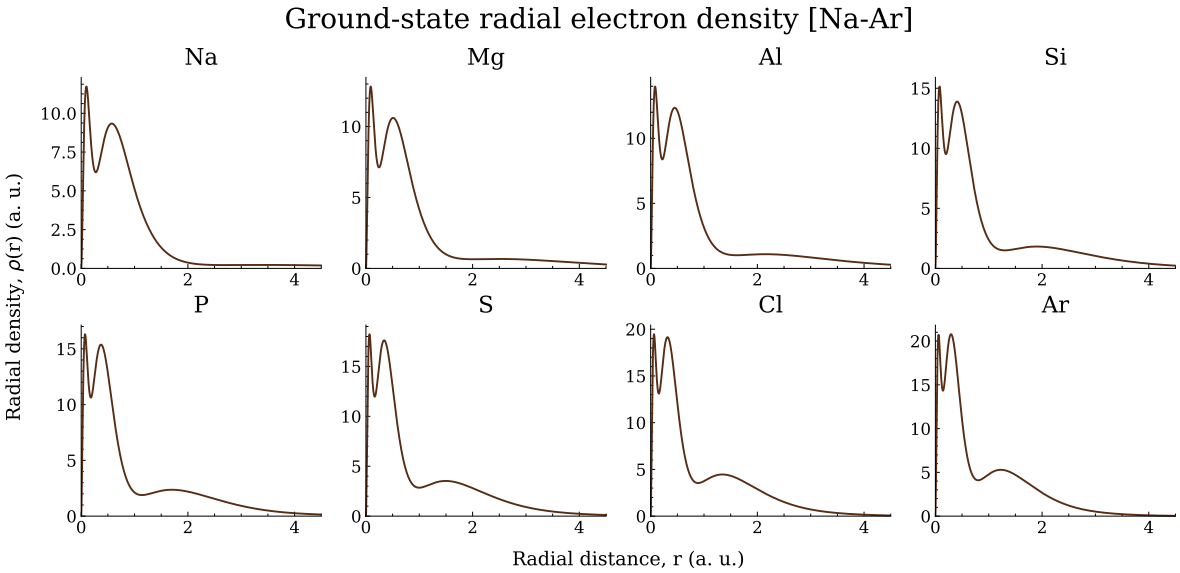

Figure 9: electron densities for neutral atoms with $Z \in [11, 18]$. The area under the curves corresponds to the number of electrons N of the system.

As expected, a third region further from the nucleus appears for the third-period elements in Figure 9.

On the other hand, Figure 8 reveals the ground-state electronic configuration of some fourth-period neutral atoms. Bearing in mind the big skip of 10 elements that lie between Ca and Ga, we see that the preceding electronic structure of Ar is still maintained. The most relevant change and unexpected at the same time is the exchange in energy between the $4s$ and $3d$ orbitals. The electronic configuration of calcium is Ca: $1s^2\ 2p^6\ 3s^2\ 3p^6\ 4s^2$ but from Ga to Kr, and assuming that the building principle holds, the unoccupied $3d$ orbitals fall below the $4s$ in energy, giving a configuration of X: $1s^2\ 2p^6\ 3s^2\ 3p^6\ 3d^{10}\ 4s^2\ 4p^n$. This trend not only differs from the $n + l$ rule but also reveals a swap between the energy content of these orbitals as $E(4s) < E(3d)$ for Ca but $E(3d) < E(4s)$ from Ga on.

We shift our attention now towards the elements left unattended, Fe through Zn, to better understand this phenomenon.

5.2.1 Transition metals

We have studied so far atomic systems that have either s or p-valence electrons. The range covering $Z \in [21, 31]$ or Sc-Zn is interesting since as long as the $n + l$ rule is fulfilled, it is expected that these elements will manifest d-valence orbitals. Furthermore, we would also like to explain the energy swap between the $4s$ and $3d$ orbitals.

Assuming the $n + l$ rule holds, the foregoing elements and their ions should have a [Ar] $4s^2\ 3d^n$ electronic with $n = N - 20$ and N the number of electrons in the system. It will also be assumed that the general rules that we have found for the multiplicities are held and that the maximum spin multiplicity available corresponds to the ground state. The results obtained for the ionization energies do not become as satisfactory as the previous ones in Figures 5 and 6.

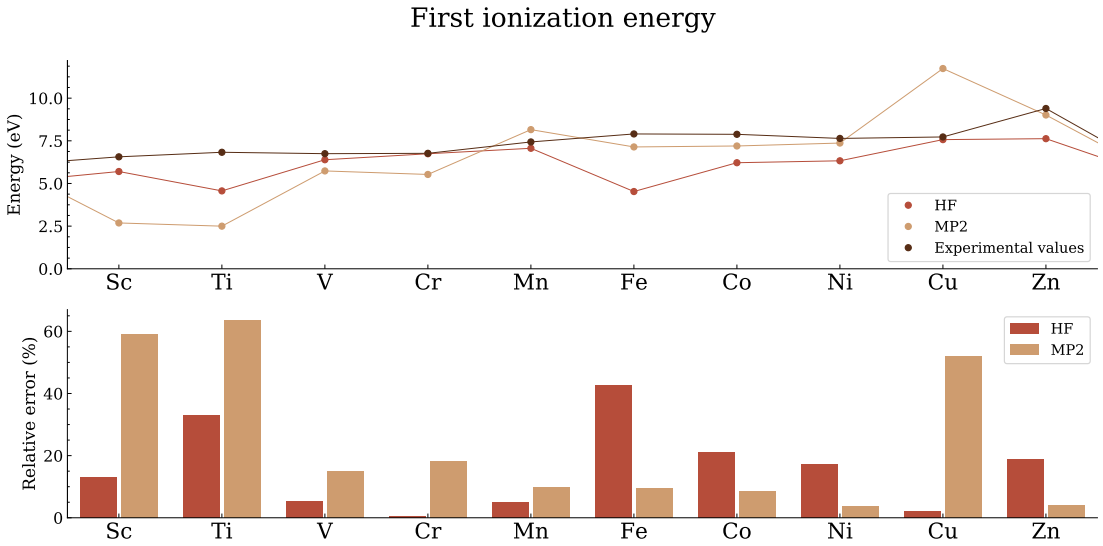

Figure 10: first ionization energies for $Z \in [21, 31]$ for HF(aug-cc-pvdz) and MP2(aug-cc-pvdz) calculations. The results are compared with the experimental data [15] and the relative error is plotted.

The most disturbing fact lies in the worse predictions for the MP2 method in comparison to the plain HF for some atoms. Furthermore, the predictions were usually lower than the experimental values, which raises even more doubts about the validity of the results. Finally, predictions for the Ti, Sc and Cu atoms in particular are clearly deficient. We must question then one of the previous assumptions, which, although have been able to reproduce the energies for alkalies, alkaline-earths and p-valence atoms, cannot explain the transition metals' ionization energies.

This instance is presented purposefully to highlight the importance of the first step followed back in Table 1. The approach followed to solve this problem consists of relaxing the fulfillment of the first Hund's rule to question the ground-state multiplicity.

The study is now restarted in order to try all possible configurations for the d electrons. We will also consider that the $4s$ orbitals do not have to be filled as they are relatively close to the d orbitals energy-wise. Let's take Z=23, vanadium, V, for instance. According to the $n + l$ rule, which is yet to be confirmed for these elements, its electronic configuration would be V: $[Ar]\ 4s^2 3d^3$. The total number of electrons that have complete freedom to

locate themselves in the 1+5 orbitals available with spin $|\uparrow\rangle$ or $|\downarrow\rangle$ is 5. Given the spin multiplicity $g = (2S + 1)$, there are 3 possibilities: doublets for $S = 1/2$, quartets for $S = 3/2$ or sextets for $S = 5/2$.

A HF calculation is performed using an inexpensive basis set 6-31g so as to evaluate the true ground state of each atom and ion. Again, as the HF calculation is a variational based method, the lowest energy configuration will be considered the atomic/ionic ground state. In those cases where the difference between them is relatively small ($\leq$ 0.025 Ha), a second calculation will be carried out using a larger basis set (aug-cc-pvtz) to verify the first result. This is done because fluctuations could stem from the basis set choice. The results for both neutral atoms and first ions are given in Table 2. We use different colours to differentiate them[23].

Table 2: ground-state energies for atoms and first cations for 4^{th}-period transition metals for a HF(6-31g). The spin multiplicity was constrained to find the most stable configuration. In those cases where the first calculation does not provide a difference of at least 0.02 Ha=0.544 eV, a HF(aug-cc-pvdz) is performed whose results are noted right under the first in the same cell.

	Neutral atom: ■				**First ion:** ■		
	Singlet	**Doublet**	**Triplet**	**Quartet**	**Quintet**	**Sextet**	**Septet**
Sc	-759.4105 -759.4728	**-759.6143**	**-759.4336** **-759.5147**	-759.5195	-	-	-
Ti	-848.0010	-848.0853 -848.1921	**-848.0989**	**-848.0872** **-848.1924**	-847.7153	- -	- -
V	-942.4085	-942.7286	-942.5533 -942.6555	**-942.7856**	**-942.5476** **-942.6750**	-942.7415	- -
Cr	-1043.0255	-1042.8736	-1043.1100	-1042.9477	-1043.1919 -1043.3169	**-1042.9915**	**-1043.1922** **-1043.3561**
Mn	-1149.1700	-1149.5444	-1149.3478	-1149.5947	-1149.4673	**-1149.7221**	**-1149.5045**
Fe	-1262.0762	-1261.9224	-1262.1738	-1262.0082	**-1262.2670**	**-1262.0372**	-
Co	-1380.7395	-1381.0233	-1380.8598	**-1381.1978**	**-1380.9568**	-1381.1303	-1380.7066
Ni	-1506.1353	-1506.2711	**-1506.6096**	**-1506.3579**	-1506.5331	-1506.0670	-
Cu	**-1638.3528** **-1638.7266**	**-1638.5670** **-1638.9626**	-1638.3774 -1638.6859	-1638.5585 -1638.8770	-1638.0542	-	-
Zn	**-1777.4828**	**-1777.2109**	-1777.3874	-1776.8058	-	-	-

The special case of Ti^+ is worth highlighting. The energies for both the doublet and quartet are almost equal and therefore, naming any of those as the true ionic ground state only with these results would be a rather bold statement. This fact has been checked with other basis sets and the quartet is proven to be the lowest energy configuration[24] consistently. Table 2 shows the differences between the predicted multiplicities according to the $n + l$ and Hund's rules and those of the lowest-energy computational states.

[23] As all atoms differ on one electron to their respective first cation, the spin multiplicity cannot be the same for both as shown in Figure 1. Table 2 is analogous but both ion and neutral atom share the same multiplicity axis.

[24] Using the aug-cc-pvdz basis we find energies of E=-848.1688 Ha and E=-848.1906 Ha for the doublet and quartet respectively.

Table 3: a comparison between the expected, obtained and reference [15] values for the spin multiplicity for the atomic and ionic ground state of the 4^{th}-period transition elements.

		Sc	Ti	V	Cr	Mn	Fe	Co	Ni	Cu	Zn
2S+1	$n+l$ and Hund's rules	2	3	4	5	6	5	4	3	2	1
	Computational	2	3	4	7	6	5	4	3	2	1
	Reference	2	3	4	7	6	5	4	3	2	1
		Sc^+	Ti^+	V^+	Cr^+	Mn^+	Fe^+	Co^+	Ni^+	Cu^+	Zn^+
2S+1	$n+l$ and Hund's rules	1	2	3	4	5	6	5	4	3	2
	Computational	3	4	5	6	7	6	5	4	1	2
	Reference	3	4	5	6	7	6	3	2	1	2

Calculations HF(aug-cc-pvdz) and MP2(aug-cc-pvdz) are repeated over the minimum energy configurations employing the same basis set. The results greatly improved the first set of predictions for the ionization energy:

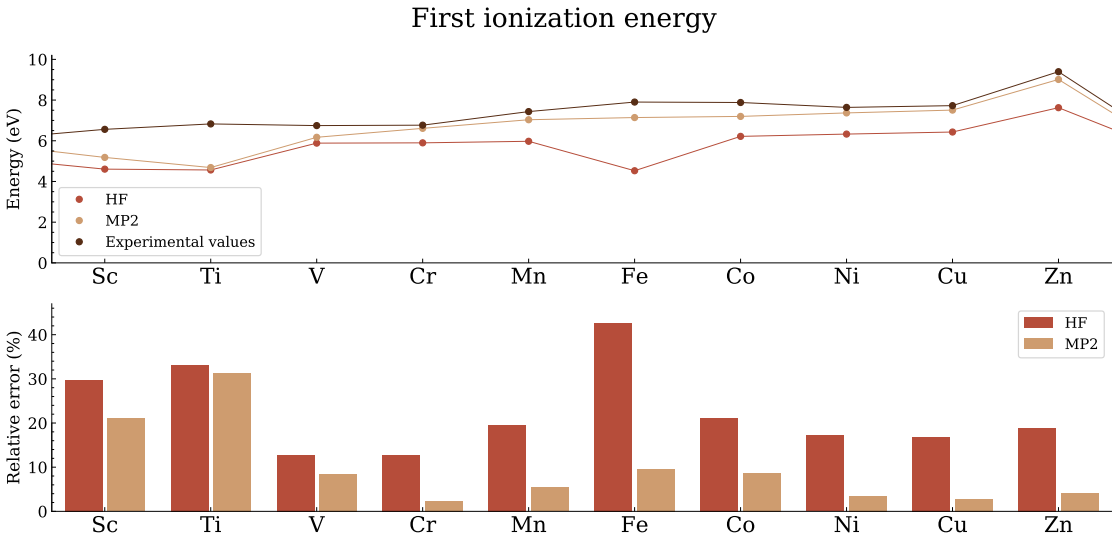

Figure 11: first ionization energies for $Z \in [21, 31]$ for a HF(aug-cc-pvdz) and MP2(aug-cc-pvdz). The results are compared with the experimental data [15]. The relative error is also analysed.

There are still some inaccuracies for the Sc and Ti atoms but the improvement is quite apparent. It is critical to notice that the multiplicities that are not in agreement in Table 3 correspond to the worse predictions for the ionization energies in Figure 10 and now fixed in Figure 11. Despite this, Sc and Ti results fail to be completely satisfactory. In addition, Co^+ and Ni^+ multiplicities are not in agreement with the reference in Table 3 but the predictions in Figure 11 are quite accurate. In order to shed some light on the causes, the occupation diagrams for these elements are shown in Figure 12.

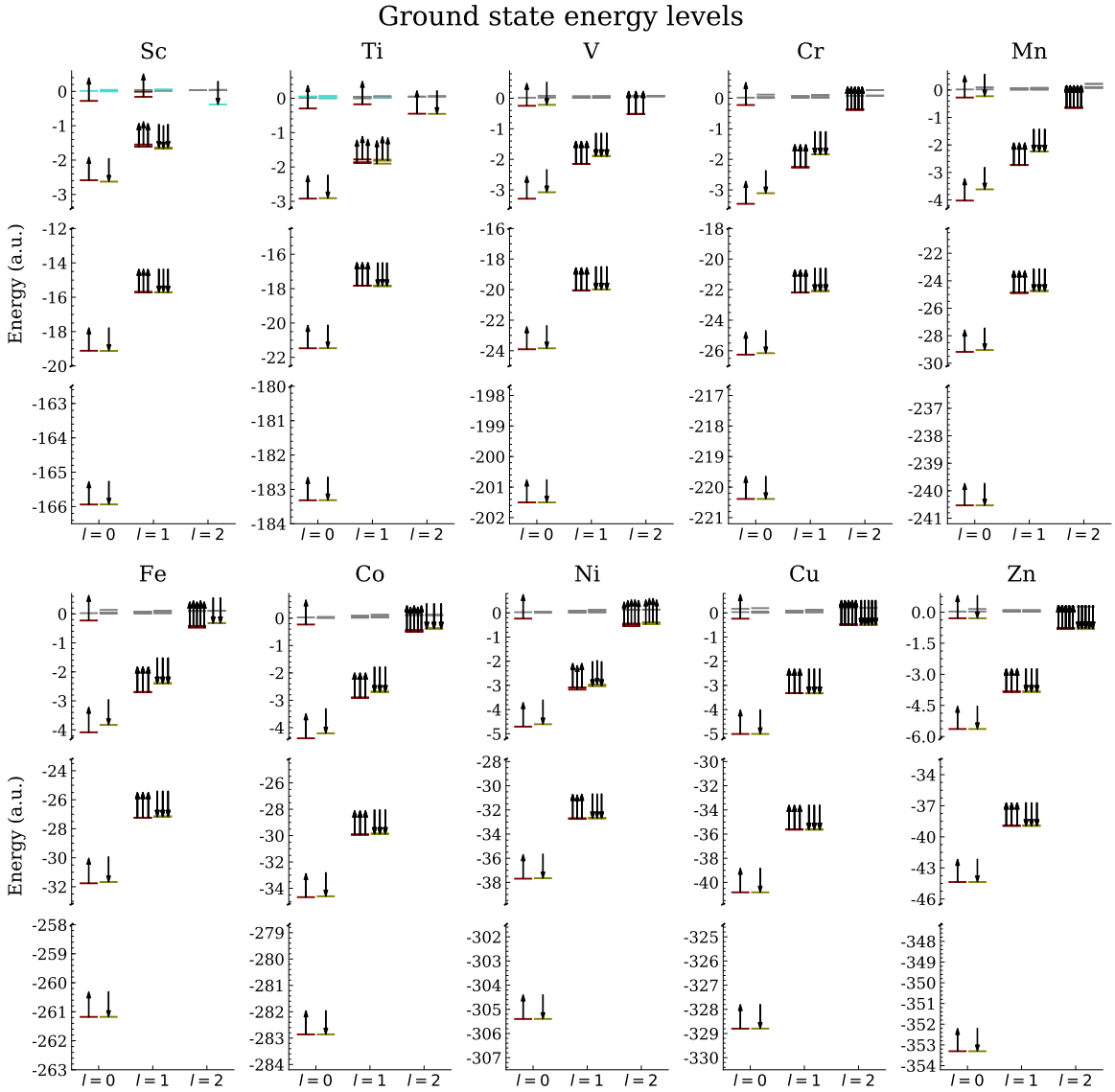

Figure 12: orbital filling for the ground states of the 4^{th} period transition metals for a HF(aug-cc-pvdz)$_c$ calculation. The monoelectronic orbitals are sorted into 3 columns according to their angular momentum $l \in \{0, 1, 2\}$. The orbitals marked in grey are unoccupied or virtual (E>0). Orbitals marked in blue do not have their orbital angular momentum l well-defined.

First of all, we will shift our attention to the Sc and Ti atoms. The potential is not close to being central or at least, the basis set employed fails to capture it. This is shown by the orbitals marked in blue in the diagram. These do not have a well-defined angular momentum l; those in the columns **l=0** or **l=2** are a linear combination between s and d-type primitives while those in the **l=2** column stem from p and f-type primitive combinations. Changes in the basis set choice eliminate the mixing but the predictions shown in Figure 11 worsen. In addition, the configurations for these atoms show the filling of 4p orbitals, which is not followed by any other transition metal, opposite to the behaviour we have repeated throughout the study: **the preceding electronic configuration is maintained as new electrons fill the unoccupied orbitals.**

A different approach was tested by increasing the accuracy of the initial guess for the orbitals until 1e-15 Ha. This allowed the configuration to readjust to give an Sc: [Ar] $3d^2$

4s and Ti: [Ar] $3d^3$ 4s, but the ionization energy values again worsen from 5.182 eV to 3.931 eV for Sc, being the experimental value 6.561 eV; and from 4.684 eV to 2.410 eV for Ti, being 6.828 eV the reference. Finally, if the reader focuses on the Sc level diagram, they will see that the ↑ electrons fill more energetic orbitals than their ↓ counterparts. All these facts make the configurations unreliable.

Following the analysis, the V atom has the expected configuration, but the $3d$ orbitals lie below the $4s$ as far as the energy is concerned. Cr is another representative of the preference that the electrons have to share the same m_s. This makes one electron in the $4s$ subshell occupy the last spot with $m_s = 1/2$ in the $3d$ subshell. After Mn, which also has the expected configuration, the $4s \downarrow$ electron falls to the $3d$ subshell until it is completed at Zn.

However, after several calculations, we must conclude that the exact electronic configuration cannot be solved with this methodology. Due to the energetic proximity between the $4s$, $4p$ and $3d$ subshells, the underlying configuration is strongly basis-dependent. For instance, the 6-31g* basis sometimes yields a filled $4s$ subshell followed by the filling of the $3d$ subshell while keeping good predictions for the ionization energies. Different basis sets from different families have been tried in addition to the tuning of the accuracy without consistent results. Sc and Ti keep being predicted to allocate electrons in 4p subshells although the quantum number l is well-defined in many calculations. The best correlations with experiments showed in Figure 6 are the ones presented in the foregoing Figure 12. The fact that $E(3d) \approx E(4s)$ also explains why good results are obtained for Co and Ni ionization energies even though the Co^+ and Ni^+ multiplicities were not predicted correctly.

The ionized electron varies depending on the atom, sometimes leaving the atom with an unpaired $4s$ electron and others leaving the $4s$ subshell empty. Ions for which all electrons are located in the $3d$ subshell are V^+, Cr^+ and Cu^+. All configurations can be found in Table 7 in the next section.

A general result that can be extracted from the trials is the following: if two subshells (4s, 4p or 3d) are filled simultaneously, the energy order for a HF calculation is always $E(3d) < E(4s) < E(4p)$. This is independent of the chosen basis set. Figure 13 shows the monoelectronic energies plotted in Figures 2, 7, 12 and 8 as a function of the atomic number Z.

We highlight that for transition metals, the $4s$ subshell is filled or half-filled while the $3d$ subshell is incomplete. The results show that the unoccupied $3d$ levels are higher in energy than the $4s$ occupied levels. This comes to show that when the valence electrons have multiple free orbitals of similar energy content, the $n + l$ rule is no longer reliable. What is more, the ionic configurations are consistently showing unpaired electrons in the $4s$ subshell at best. If the ordering $4s \rightarrow 3d$ held, the $4s$ subshell should be kept intact.

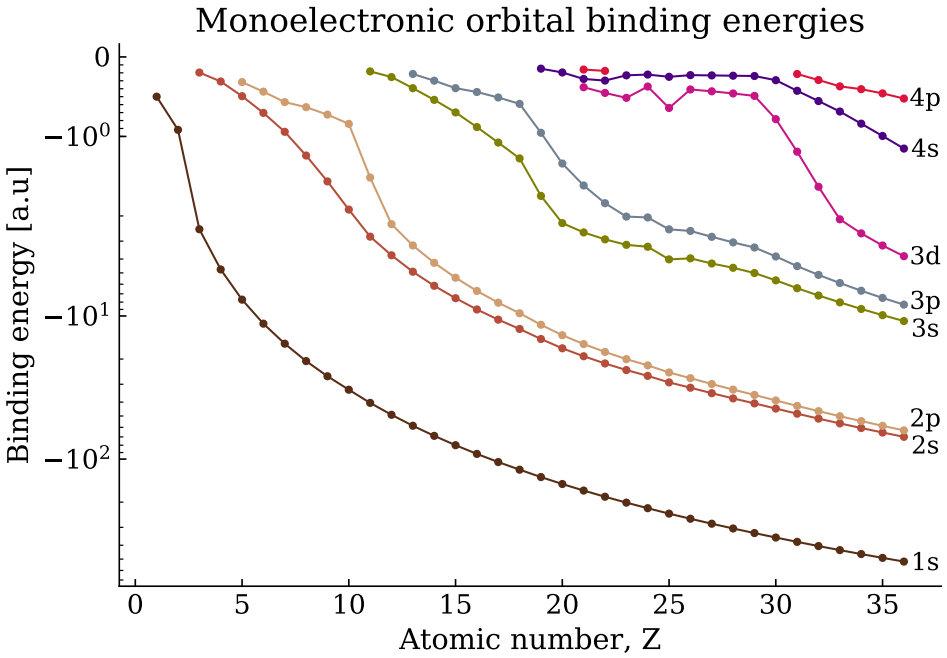

Figure 13: comparison of the monoelectronic binding energies for neutral atoms of the first four periods. Given the fact that these energies are not constant as seen in Figures 2, 7 and 8, the mean value of occupied orbitals for each class is plotted. This graphic was inspired in [16], p. 55.

5.3 Electron affinities

The last atomic property we tried to predict is the electron affinity. This magnitude is defined as the amount of energy released in the reaction:

$$X + e^- \longrightarrow X^- + \text{energy} \quad , \tag{5.3}$$

where X is the chemical symbol of the element with atomic number Z. A positive electronic affinity will be understood as an exothermic reaction, while a negative value will mean that some energy is required in order to bound the electron.

It will again be necessary to split the study and discuss the d-valence electrons separately. The procedure will be the same as for the ionization energies, that is computing the HF and a subsequent MP2 in an attempt to obtain better quantitative results.

The basis set choice is something especially important for negatively charged chemical species because of the loose bounded electrons. The absolute values for the electronic affinities of a given atom are lower than their ionization energies according to experiments [17]. Again, a higher energy associated with a monoelectronic orbital is related to a distant presence probability from the nucleus and sometimes diffuse primitives are mandatory to obtain reasonable results. Let's take the F atom for instance and compare the effect of including a diffuse function in the already familiar 6-311g* basis, that is the 6-311+g* basis set, in the ground-state energy.

The double valence correlation-consistent basis sets have also been added in Table 4 in order to justify the final choice.

Table 4: a comparative view of ionic and atomic energies with 6-311g* and cc-pvdz basis sets and their diffuse expansion for F. The computational and experimental values for the ionization energy and electron affinity are also noted.

Basis set	Method	Ion. energy (eV)	Elec. aff. (eV)	Cation (Ha)	Atom (Ha)	Anion (Ha)
6-311g*	HF	15.6829	0.1693	-98.82056	-99.39689	-99.40312
	MP2	16.9200	1.6180	-98.95933	-99.58113	-99.64059
6-311+g*	HF	15.7022	1.2466	-98.82289	-99.39994	-99.44575
	MP2	17.0030	3.2470	-98.96142	-99.58627	-99.70559
cc-pvdz	HF	15.6388	-0.2395	-98.80061	-99.37533	-99.36653
	MP2	16.7900	1.0757	-98.90450	-99.52152	-99.56105
aug-cc-pvdz	HF	15.7249	1.2712	-98.80393	-99.38181	-99.42852
	MP2	17.1404	3.5488	-98.91463	-99.54453	-99.67494
Experimental values		17.42282	3.401	-	-	-

The first result drawn from Table 4 is the fact that the atomic and positive-ion HF energies, which always constitute a high bound for the real energy, do not show great sensitivity to the addition of diffuse functions. The energies of anions on the other hand present variations of $\sim 5 \cdot 10^{-2}$ Ha ≈ 1.4 eV, improving this boundary limit. This has a direct effect on the electron affinity predictions, which, as expected, yield very poor results unless diffuse functions are included. What is more, given the relatively low values for this magnitude, the MP2 perturbation is almost mandatory to approach the reference [17].

The electron affinities for atoms H-Kr were calculated using a HF(aug-cc-pvdz) and MP2(aug-cc-pvdz) assuming that anions followed the $n + l$ and Hund's rules and compared to the reference values in Figure 14.

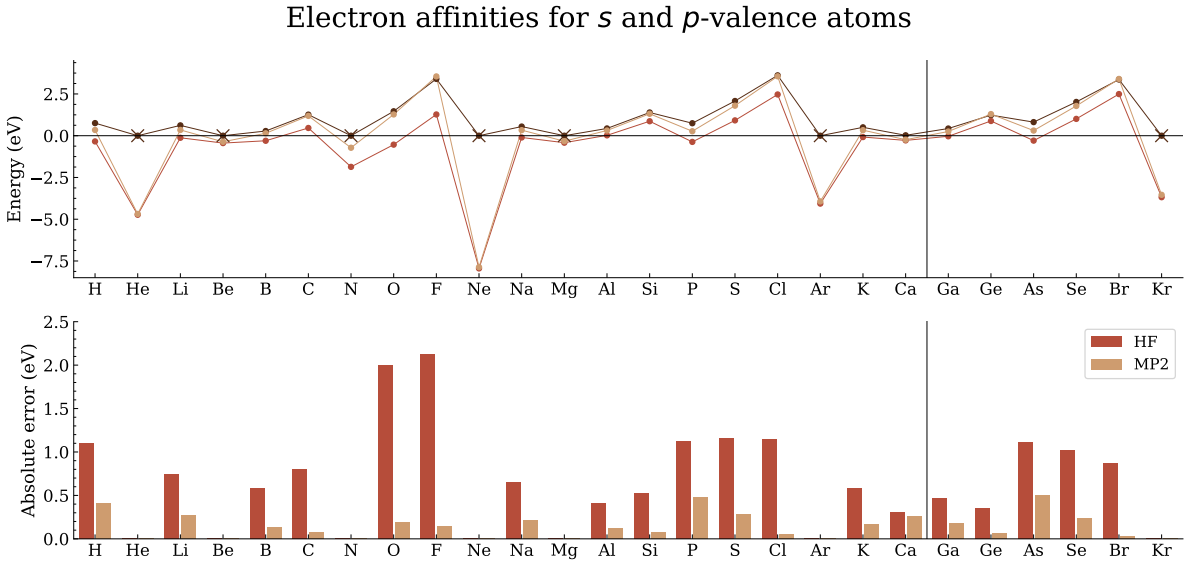

Figure 14: electron affinities according to HF(aug-cc-pvdz)$_c$ and MP2(aug-cc-pvdz) calculations for atoms H-Kr excluding the transition elements. The alkalies and Ca are exceptions as the aug-pc-3 basis sets was used instead. Those atoms whose electronic affinity cannot be measured experimentally since reaction 5.3 is not favourable energetically speaking have their reference values [17] [18] crossed.

Firstly, it becomes apparent that the HF method is generally insufficient to predict exothermic reactions for most atoms. The MP2 calculations on the other hand yield good approximations for the experimental values, especially for halogens and 14^{th}-group atoms (C, Si and Ge). Moreover, electron affinities for these atoms are higher compared to their immediate neighbourhood, which comes to support the statement on how filled and half-filled subshells constitute remarkably stable configurations.

As noted in the Figure 15 caption, the aug-cc-pvdz basis was not enough to accurately describe the electron affinities for some specific systems, the Na and Li. For that reason, the aug-pc-3 basis set was selected to tackle the calculations. These elements have low electron affinities that can become difficult to simulate without employing larger basis sets. Finally, the aug-cc-pvdz basis is not available for K and Ca, so the same alternative was tried given the good results it showed for the other two alkalies.

Table 5: variation of the MP2(aug-cc-pvdz) and MP2(aug-pc-3) energy for Li and Na atoms and their first anions in Ha. The predicted electron affinities and reference values [17] are also noted in eV.

	Li	**Li^-**	**Elec. aff. (eV)**	**Ref. (eV)**
aug-cc-pvdz	-7.43356	-7.35539	-2.1271	0.618
aug-pc-3	-7.45083	-7.46350	0.3448	
	Na	**Na^-**	**Elec. aff. (eV)**	**Ref. (eV)**
aug-cc-pvdz	-161.85597	-161.77710	-2.1460	0.434
aug-pc-3	-161.96951	-161.98175	0.3331	

Unusual configurations are predicted for some anions. For instance, the ion Ca^- is predicted to be Ca^-: [Ar] $4s^2$ 5s while Kr^- has a configuration Kr^-: [Kr] 5p, instead of the expected Ca^-: [Ar] $4s^2$ 3d and Kr^-: [Kr] 5s.

The transition metals entitled to serious complications. All the basis sets discussed in this work fail to provide satisfactory results for the electron affinities. Figure 15 shows a great mismatch between the experimental and computational results. The anion configuration is assumed to fulfill the $n + l$ and Hund's rules. The aug-pc-3 basis set was used for the Cu^- as it fitted better the experimental values.

Only the Zn^- and Cu^- ions seem to yield reliable results. A closer look at the electronic configuration regarding Mn^- reveals a [Ar] $3d^4$ 4s $4p^3$. We consider the electronic affinity of $\approx$ 20 eV too big to think that this configuration is correct. The Cu^- on the other hand gives a [Ar] $3d^4$ $4s^2$ $4p^6$. Again, the preference to occupy the $4p$ orbitals appears for transition metals. Only Zn^- has a reasonably expected configuration [Ar] $3d^{10}$ $4s^2$ 4p.

The availability of a high number of energy levels ($10d$+$2s$+$6p$) with similar energies makes the calculations extremely sensitive to the initial guesses and the basis set choice. However, in practical scenarios, it would be unlikely to find negative ions of these atoms in particular. We consider this as the reason why all the basis sets fail to describe them.

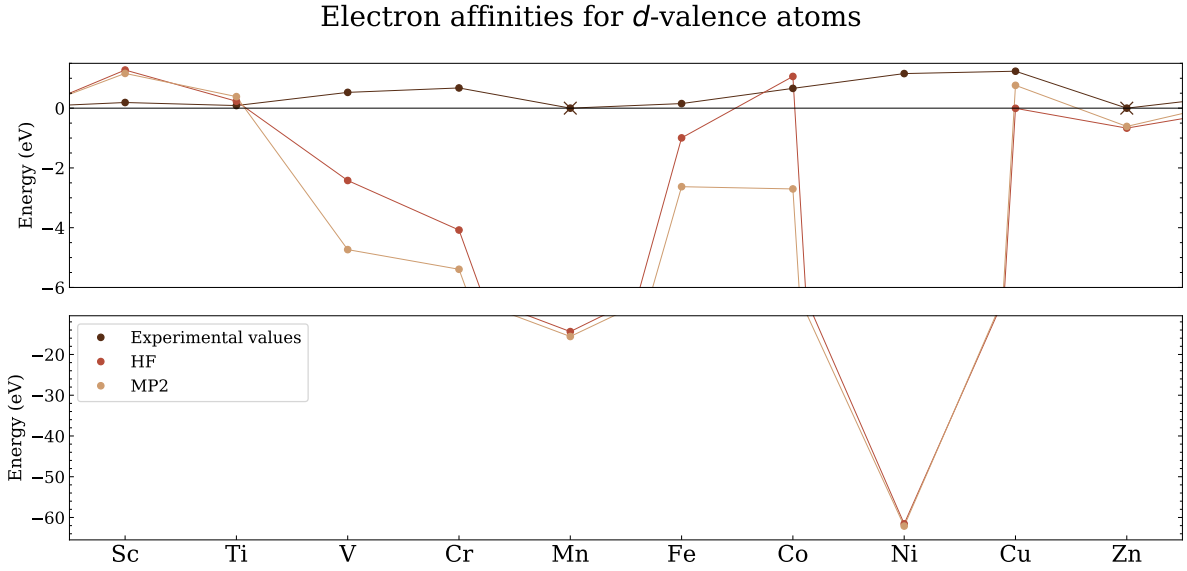

Figure 15: electron affinities for HF (aug-cc-pvdz) and MP2 (aug-cc-pvdz) calculations for the fourth period transition metals Sc-Zn, excepting Cu, for which the aug-pc-3 basis set was used instead.

6 Conclusions

Se concluye con una recopilación de los resultados más relevantes del estudio y una crítica a la precisión del método empleado. Se intentan corregir algunos resultados en desacuerdo con la referencia mediante un cálculo DFT y por último se indican posibles continuaciones al trabajo desarrollado.

This study has shown the strong capabilities of computational algorithms in order to simulate the electronic structure of atoms. These methods are nonetheless applicable to molecules under the Born-Oppenheimer approximation. In fact, the molecular initial guess for the orbital occupation is a linear combination of atomic orbitals (LCAO), so this study constitutes a good starting point for an extension to molecular calculations. This work has made use of the free-distribution software package NWCHEM.

Through the entirety of the analysis, the MP2 calculations have provided as expected better estimations for the ionization energies than the HF method. The accuracy of the predictions ($<$ 1 eV even for the worst results) constitutes a great preliminary description of the system's properties at a low computational cost without even considering relativistic effects. In this study, we have employed this comparison in order to verify the electronic structure of the first 4 rows of the periodic table.

The Aufbau Principle has also been verified for the s and p-valence atoms but some remarks must be made for the d-valence atoms. This study has shown that the $4s$ orbital is consistently higher in energy than the $3d$ orbital for HF calculations. Therefore, when the d-subshell is not completely filled, the unoccupied d-orbitals lie above in energy than the $4s$. In other words, the complete set of 5 d-type orbitals do not work as a whole, but the differences in energy are high enough to let another set of orbitals, the $4s$ in this case, to be allocated between them energetically speaking.

In this regard, the existence of multiple levels with similar energies makes the resolution of the electronic structure much more challenging. The electronic configuration becomes extremely basis-dependent if most of those levels are unoccupied. This is why the electron configuration for Sc and Ti in Figure 12 is not reliable for valence electrons even though they give the best result among the basis sets discussed in this project for the ionization energies. We have demonstrated the importance of the diffuse functions in low-bounded electron systems for energy predictions.

As we have said, the fidelity range that we conclude the MP2 calculations have for the atomic systems is at least $\sim$ 0.8 eV in the worst cases if usual split-valence or correlation-consistent basis are used, although the accuracy is generally higher. Therefore, the prediction of energetic processes below this threshold should be treated with special care. However, we have obtained even better results for the electron affinities of *s* and *p*-valence atoms.

On the other hand, this approach has failed to describe the electron affinities for Sc-Zn, which were already extremely sensitive without adding an extra electron to the system, excepting the Zn, that has filled $3d$ and $4s$ subshells. This leaves no choice for new electrons but to occupy $4d$ orbitals.

In an attempt to solve the problems that Sc and Ti posed, a DFT calculation was explored keeping the multiplicities given in Table 2. We shall not explain the full principle behind the DFT theory and Kohn-Sham equations, but in short, the energy is treated as a functional of the electron density instead of the wave function as in the HF method. The LSDA[25] and Vosko-Wilk-Nusair (VWN) correlation potential were used for the calculations[26]. The results predict the correct configurations Sc: [Ar] $4s^2$ 3d and Ti: [Ar] $3d^2$ $4s^2$. Again, the ionization leaves the 4s subshell half-filled. The degree of accuracy for the ionization energy predictions matches the one obtained with the HF/MP2 theories:

Table 6: comparison of the results obtained for the MP2(aug-cc-pvdz)$_c$ and DFT-LSDA methods with the same basis.

	ΔI_{MP2} (eV)	ΔI_{DFT} (eV)	ΔI_{exp} (eV)
Sc	5.182	6.482	6.561
Ti	4.684	6.475	6.828

Regarding the $3d \rightarrow 4s$ filling order, the DFT confirms the results obtained with the HF method for Ti but not for Sc. However, as the *d*-subshell is being filled by electrons, the gap between the levels increases just as Figure 13 indicates so the $3d$ orbitals are preferred in the long term.

The final electronic structure of the studied atoms and ions as well as the spin multiplicities are noted in Table 7.

Natural continuations of this study would be the extension to DFT or Coupled Cluster[27] methods (see Tensor Contraction Engine in the manual [13]). It would be extremely

[25]Local spin-density approximation.
[26]These are the default options in NWCHEM for DFT calculations.
[27]This is another post-HF method to estimate the correlation energy.

interesting to include relativistic corrections since the spin-orbit coupling term becomes more important as the number of electrons grows. In fact, for larger atoms, the basis sets used in the study are replaced by their relativistic versions. The accountancy of these terms is expected to correct the odd configurations for Ca^- and Kr^-. Another possible path would involve the extension to diatomic molecules to study the effect of close nuclei on the orbital shape and energy.

Table 7: spin multiplicities and ground-state electron configurations for the atoms, cation and anions from H to Kr. The results correspond to a HF(6-311g*) for s and p-valence atoms their cations and a HF(aug-cc-pvdz) for Fe-Zn, their cations and for all anions (excepting alkalies and Ca^- for which a HF(aug-pc-3) was chosen). Those configurations in bright red correspond to the estimations extracted from the DFT. The low bounded electrons for the negative ions of Sc-Cu were not able to be reproduced satisfactorily. The results are compared with the NIST Database [15] reference. In case of a mismatch, the reference is written explicitly and the wrong configuration highlighted in blue.The inversion $4s3d \rightarrow 3d4s$ is not considered a mismatch. Unexpected terms for anions are marked in blue as well.

Atom	2S+1	Elec. Conf.	Reference	Cation	2S+1	Elec. Conf.	Reference	Anion	2S+1	Elec. Conf.
H	2	1s	✓	H^+	-	-	-	H^-	1	$1s^2$
He	1	$1s^2$	✓	He^+	2	1s	✓	He^-	2	[He]2s
Li	2	[He]2s	✓	Li^+	1	$1s^2$	✓	Li^-	1	$[He]2s^2$
Be	0	$[He]2s^2$	✓	Be^+	2	[He]2s	✓	Be^-	2	$[He]2s^2p$
B	2	$[He]2s^2p$	✓	B^+	1	$[He]2s^2$	✓	B^-	3	$[He]2s^2p^2$
C	3	$[He]2s^2p^2$	✓	C^+	2	$[He]2s^22p$	✓	C^-	4	$[He]2s^2p^3$
N	4	$[He]2s^2p^3$	✓	N^+	3	$[He]2s^22p^2$	✓	N^-	3	$[He]2s^22p^4$
O	3	$[He]2s^2p^4$	✓	O^+	4	$[He]2s^22p^3$	✓	O^-	2	$[He]2s^22p^5$
F	2	$[He]2s^2p^5$	✓	F^+	3	$[He]2s^22p^4$	✓	F^-	1	$[He]2s^22p^6$
Ne	1	$[He]2s^2p^6$	✓	Ne^+	2	$[He]2s^22p^5$	✓	Ne^-	2	[Ne]3s
Na	2	[Ne]3s	✓	Na^+	1	$[He]2s^22p^6$	✓	Na^-	1	$[Ne]3s^2$
Mg	1	$[Ne]3s^2$	✓	Mg^+	2	[Ne]3s	✓	Mg^-	2	$[Ne]3s^23p$
Al	2	$[Ne]3s^23p$	✓	Al^+	1	$[Ne]3s^2$	✓	Al^-	3	$[Ne]3s^23p^2$
Si	3	$[Ne]3s^23p^2$	✓	Si^+	2	$[Ne]3s^23p$	✓	Si^-	4	$[Ne]3s^23p^3$
P	4	$[Ne]3s^23p^3$	✓	P^+	3	$[Ne]3s^23p^2$	✓	P^-	3	$[Ne]3s^23p^4$
S	3	$[Ne]3s^23p^4$	✓	S^+	4	$[Ne]3s^23p^3$	✓	S^-	2	$[Ne]3s^23p^5$
Cl	2	$[Ne]3s^23p^5$	✓	Cl^+	3	$[Ne]3s^23p^4$	✓	Cl^-	1	$[Ne]3s^23p^6$
Ar	1	$[Ne]3s^23p^6$	✓	Ar^+	2	$[Ne]3s^23p^5$	✓	Ar^-	2	[Ar]4s
K	2	[Ar]4s	✓	K^+	1	$[Ne]3s^23p^6$	✓	K^-	1	$[Ar]4s^2$
Ca	1	$[Ar]4s^2$	✓	Ca^+	2	[Ar]4s	✓	Ca^-	2	$[Ar]4s^25s$
Sc	2	$[Ar]4s^23d$	✓	Sc^+	3	[Ar]4s3d	✓	Sc^-	?	?
Ti	3	$[Ar]3d^24s^2$	✓	Ti^+	4	$[Ar]3d^24s$	✓	Ti^-	?	?
V	4	$[Ar]3d^34s^2$	✓	V^+	5	$[Ar]3d^4$	✓	V^-	?	?
Cr	7	$[Ar]3d^54s$	✓	Cr^+	6	$[Ar]3d^5$	✓	Cr^-	?	?
Mn	6	$[Ar]3d^54s^2$	✓	Mn^+	7	$[Ar]3d^54s$	✓	Mn^-	?	?
Fe	5	$[Ar]3d^74s$	$[Ar]3d^64s^2$	Fe^+	6	$[Ar]3d^64s$	✓	Fe^-	?	?
Co	4	$[Ar]3d^84s$	$[Ar]3d^74s^2$	Co^+	5	$[Ar]3d^74s$	$[Ar]3d^8$	Co^-	?	?
Ni	3	$[Ar]3d^94s$	$[Ar]3d^84s^2$	Ni^+	4	$[Ar]3d^84s$	$[Ar]3d^9$	Ni^-	?	?
Cu	2	$[Ar]3d^14s$	✓	Cu^+	1	$[Ar]3d^{10}$	✓	Cu^-	1	?
Zn	1	$[Ar]3d^{10}4s^2$	✓	Zn^+	2	$[Ar]3d^{10}4s$	✓	Zn^-	2	$[Ar]3d^{10}4s^24p$
Ga	2	$[Ar]3d^{10}4s^24p$	✓	Ga^+	1	$[Ar]3d^{10}4s^2$	✓	Ga^-	3	$[Ar]3d^{10}4s^24p^2$
Ge	3	$[Ar]3d^{10}4s^24p^2$	✓	Ge^+	2	$[Ar]3d^{10}4s^24p$	✓	Ge^-	4	$[Ar]3d^{10}4s^24p^3$
As	4	$[Ar]3d^{10}4s^24p^3$	✓	As^+	3	$[Ar]3d^{10}4s^24p^2$	✓	As^-	3	$[Ar]3d^{10}4s^24p^4$
Se	3	$[Ar]3d^{10}4s^24p^4$	✓	Se^+	4	$[Ar]3d^{10}4s^24p^3$	✓	Se^-	2	$[Ar]3d^{10}4s^24p^5$
Br	2	$[Ar]3d^{10}4s^24p^5$	✓	Br^+	3	$[Ar]3d^{10}4s^24p^4$	✓	Br^-	1	$[Ar]3d^{10}4s^24p^6$
Kr	1	$[Ar]3d^{10}4s^24p^6$	✓	Kr^+	2	$[Ar]3d^{10}4s^24p^5$	✓	Kr^-	2	$[Ar]3d^{10}4s^24p^65p$

References

[1] B. H. Bransden and C. J. Joachain, *Physics of atoms and molecules*. Longman Scientific & Technical and John Wiley & Sons Inc., 1983.

[2] Chr. Møller and M. S. Plesset, "Note on an Approximation Treatment for Many-Electron Systems," *Physical Review*, vol. 46, pp. 618–622, Oct. 1934.

[3] C. J. Cramer, *Essentials of Computational Chemistry: theories and Models*. Chichester, Essex: John Wiley & Sons, Ltd, 2 ed., 2004.

[4] C. Cohen-Tannoudji, B. Diu, and F. Laloë, *Quantum Mechanics*, vol. 2, ch. IX. Paris: Heinemann, 1973.

[5] C. Cohen-Tannoudji, B. Diu, and F. Laloë, *Quantum Mechanics*, vol. 1, ch. VII. Paris: Heinemann, 1973.

[6] W. J. Hehre, R. F. Stewart and J. A. Pople, "Self-Consistent Molecular-Orbital Methods. I. Use of Gaussian Expansions of Slater-Type Atomic Orbitals," *J. Chem. Phys.*, vol. 51, no. 6, pp. 2657–2664, 1969.

[7] R. Ditchfield, W. J. Hehre and J. A. Pople , "Self-Consistent Molecular-Orbital Methods. IX. An Extended Gaussian-Type Basis for Molecular-Orbital Studies of Organic Molecules," *J. Chem. Phys.*, vol. 54, no. 2, pp. 724–728, 1971.

[8] W. J. Hehre, R. Ditchfield and J. A. Pople , "Self-Consistent Molecular Orbital Methods. XII. Further Extensions of Gaussian-Type Basis Sets for Use in Molecular Orbital Studies of Organic Molecules," *J. Chem. Phys.*, vol. 56, no. 5, pp. 2257–2261, 1972.

[9] Thom H. Dunning, Jr, "Gaussian basis sets for use in correlated molecular calculations. I. The atoms boron through neon and hydrogen," *J. Chem. Phys.*, vol. 90, no. 2, pp. 1007–1023, 1989.

[10] Frank Jensen, "Polarization consistent basis sets: Principles," *J. Chem. Phys.*, vol. 105, no. 20, pp. 9113–9125, 2003.

[11] M. Valiev, E.J. Bylaska, N. Govind, K. Kowalski, T.P. Straatsma, H.J.J. van Dam, D. Wang, J. Nieplocha, E. Apra, T.L. Windus, W.A. de Jong, "NWChem: a comprehensive and scalable open-source solution for large scale molecular simulations," *Computer Physics Communications*, vol. 181, pp. 1477–1489, Sept. 2010.

[12] The Molecular Sciences Software Institute (MolSSI), "Basis Set Exchange, BSE Library v0.8.13," 2020. URL: https://www.basissetexchange.org. Accessed April 24, 2021.

[13] "NWChem Manual - NWChem." https://nwchemgit.github.io/Home.html. Accessed April 24, 2021.

[14] T. Koopmans, "Über die Zuordnung von Wellenfunktionen und Eigenwerten zu den Einzelnen Elektronen Eines Atoms. (German) [About the assignment of wave functions and intrinsically to the individual electrons of an atom]," *Physica*, vol. 1, pp. 104–113, Jan. 1934.

[15] Kramida, A., Ralchenko, Yu., Reader, J., and NIST ASD Team, "NIST Atomic Spectra Database (ver. 5.8)," 2020. https://physics.nist.gov/asd. Accessed December 21, 2020.

[16] C. Sánchez del Río, *Introducción a la teoría del átomo*. Editorial Alhambra S.A., 1 ed., 1977.

[17] Russell D. Johnson III (Editor), "NIST Computational Chemistry Comparison and Benchmark Database. NIST Standard Reference Database Number 101," Aug. 2020. https://cccbdb.nist.gov. Accessed April 10, 2021.

[18] "Electron affinity (data page)." Wikipedia, the free encyclopedia. https://en.wikipedia.org/wiki/Electron_affinity_(data_page). Accessed May 14, 2021.

[19] L. A. Cabrera, L. A. Fernández, and R. Bader, *Introduction to Advanced Topics of Computational Chemistry*, ch. 1, pp. 41–70. La Habana, Cuba: Facultad de Química, Universidad de La Habana, 2003.

[20] J. Hermosa Muñoz, "Estructura electrónica y vibracional de moléculas con interés astrofísico," Master's thesis, Universidad de La Laguna, June 2018.

[21] D. G. S. Nippard, "Modelling Radial Electron Densities of Atoms in Molecules," Master's thesis, Memorial University of Newfoundland, May 2014.

[22] E. U. Condon and G. H. Shortley, *The Theory of Atomic Spectra*. Cambridge University Press, 1935.

Appendices

A Sample input file and data retrieval

In case the reader is interested in replicating the calculations discussed in this work or in starting any HF/MP2 calculation with NWChem, we attach an input file sample.

```
echo
start c_mp2
title "Carbon MP2"
charge  0
geometry
 C    0.0  0.0  0.0
end
scf
 uhf
 triplet
 maxiter 2000
end
print debug
basis cartesian
 C library 6-311g*
end
task mp2
```

This is a 2000-iteration[28] MP2(6-311g*)$_c$ calculation for neutral carbon with all the information about the initial guesses, explicit intermediate values... thanks to the `debug` printing option. This data volume is likely to be unnecessary, so just by leaving `print` or deleting the whole line. The needed HF is also performed prior to the MP2 stage using the same basis set.

Assuming the debug option is not required, the output file will consist of a preamble where the primitives are explicitly written as well as the number of contracted resulting functions. The coefficients and exponents are not normalized. This fact is not indicated in the manual [13] and must be taken into account for any external operation such as the retrieval of the radial densities. The HF calculation is then performed, showing the energy evolution throughout the iterative process. Right below, the final HF energy is displayed alongside the monoelectronic energies and the coefficients obtained for each of the orbitals. The final MP2 energy is attached at the end of the text file.

[28] This is the maximum number of iterations but the procedure may converge before.

B Additional tables

Table 8: ground-state energies for atoms and their respective first positive ions ranging from H to Ca and Ga to Kr yielded by a HF(6-311g*)$_c$ and MP2(6-311g*)$_c$ calculation and from Sc to Zn by a HF(aug-cc-pvdz)$_c$ and MP2(aug-cc-pvdz)$_c$. The estimation for the correlation energy, the predicted first ionization energies for each method (ΔI_{HF} and ΔI_{MP2}) and their experimental values (ΔI_{exp}) [15] are also noted explicitly.

	E_{HF} (a.u.)	E_{MP2} (a.u.)	E_{corr} (a.u.)		E_{HF} (a.u.)	E_{MP2} (a.u.)	E_{corr} (a.u.)	ΔI_{HF} (eV)	ΔI_{MP2} (eV)	ΔI_{exp} (eV)
H	-0.49981	-0.49981	0.00000	H^+	0.00000	0.00000	0.00000	13.6005	13.6005	13.5984
He	-2.85990	-2.87280	-0.01291	He^+	-1.99814	-1.99814	0.00000	23.4496	23.8008	24.5874
Li	-7.43212	-7.44509	-0.01297	Li^+	-7.23584	-7.24841	-0.01257	5.3412	5.3520	5.3917
Be	-14.57189	-14.61405	-0.04216	Be^+	-14.27635	-14.29089	-0.01454	8.0420	8.7937	9.3227
B	-24.53015	-24.58715	-0.05700	B^+	-24.23528	-24.28708	-0.05180	8.0240	8.1654	8.2980
C	-37.68915	-37.76495	-0.07580	C^+	-37.29199	-37.35630	-0.06431	10.8074	11.1199	11.2603
N	-54.39814	-54.49704	-0.09890	N^+	-53.88626	-53.96730	-0.08104	13.9290	14.4149	14.5341
O	-74.80526	-74.94257	-0.13731	O^+	-74.36484	-74.46680	-0.10196	11.9846	12.9463	13.6181
F	-99.39689	-99.58113	-0.18424	F^+	-98.82056	-98.95933	-0.13877	15.6829	169200	17.4228
Ne	-128.52267	-128.76113	-0.23847	Ne^+	-127.79679	-127.97983	-0.18304	19.7522	21.2604	21.5645
Na	-161.84605	-161.97775	-0.13170	Na^+	-161.66430	-161.79410	-0.12980	4.9458	4.9975	5.1391
Mg	-199.60699	-199.75886	-0.15187	Mg^+	-199.36425	-199.49257	-0.12832	6.6052	7.2461	7.6462
Al	-241.87225	-242.02909	-0.15684	Al^+	-241.66786	-241.82147	-0.15361	5.5619	5.6497	5.9858
Si	-288.85044	-289.01812	-0.16768	Si^+	-288.56980	-288.73156	-0.16176	7.6365	7.7978	8.1517
P	-340.70784	-340.89310	-0.18526	P^+	-340.34259	-340.51823	-0.17564	9.9389	10.2005	10.4867
S	-397.49847	-397.70304	-0.20456	S^+	-397.16246	-397.35339	-0.19093	9.1434	9.5144	10.3600
Cl	-459.47356	-459.63555	-0.16199	Cl^+	-459.03979	-459.18168	-0.14189	11.8036	12.3504	12.9676
Ar	-526.80683	-527.00923	-0.20240	Ar^+	-526.26831	-526.44523	-0.17692	14.6539	15.3473	15.7596
K	-599.14932	-599.42504	-0.27573	K^+	-599.00213	-599.26927	-0.26714	4.0051	4.2388	4.3407
Ca	-676.74067	-677.05213	-0.31146	Ca^+	-676.55259	-676.83959	-0.28700	5.1180	5.7835	6.1132
Sc	-759.68153	-759.84703	-0.16550	Sc^+	-759.51226	-759.65659	-0.14433	4.60607	5.18209	6.56149
Ti	-848.33654	-848.57264	-0.23610	Ti^+	-848.16879	-848.40050	-0.23172	4.56485	4.68413	6.82812
V	-942.89032	-943.21129	-0.32097	V^+	-942.67408	-942.98451	-0.31042	5.88418	6.17111	6.74619
Cr	-1043.35577	-1043.73938	-0.38362	Cr^+	-1043.13900	-1043.49646	-0.35745	5.89838	6.61035	6.76651
Mn	-1149.86823	-1150.26921	-0.40098	Mn^+	-1149.64866	-1150.01072	-0.36207	5.97477	7.03380	7.43404
Fe	-1262.38433	-1262.90067	-0.51634	Fe^+	-1262.21793	-1262.63824	-0.42031	4.52786	7.14094	7.90247
Co	-1381.36370	-1381.96089	-0.59719	Co^+	-1381.13525	-1381.69640	-0.56114	6.21626	7.19720	7.88101
Ni	-1506.82711	-1507.50883	-0.68172	Ni^+	-1506.59453	-1507.23803	-0.64350	6.32888	7.36877	7.63988
Cu	-1638.96235	-1639.76725	-0.80490	Cu^+	-1638.72606	-1639.49135	-0.76529	6.42977	7.50756	7.72638
Zn	-1777.84675	-1778.65294	-0.80619	Zn^+	-1777.56651	-1778.32172	-0.75521	7.62574	9.01290	9.39420
Ga	-1923.18223	-1923.62564	-0.44341	Ga^+	-1922.97788	-1923.41299	-0.43511	5.5605	5.7863	5.9993
Ge	-2075.27982	-2075.71910	-0.43928	Ge^+	-2075.00665	-2075.43402	-0.42738	7.4333	7.7574	7.8994
As	-2234.15408	-2234.60007	-0.44599	As^+	-2233.80662	-2234.23723	-0.43061	9.4547	9.8733	9.7886
Se	-2399.78581	-2400.24480	-0.45900	Se^+	-2399.47232	-2399.91279	-0.44047	8.5305	9.0346	9.7524
Br	-2572.35545	-2572.85334	-0.49789	Br^+	-2571.95974	-2572.43659	-0.47685	10.7678	11.3403	11.8138
Kr	-2751.96296	-2752.46125	-0.49830	Kr^+	-2751.47975	-2751.94894	-0.46919	13.1488	13.9409	13.9996

Table 9: electron affinities (ΔA) for HF(aug-cc-pvdz)$_c$ and MP2(aug-cc-pvdz)$_c$ according to the multiplicities shown in Table 7 and reference values (ΔA_{exp}) [17] [18]. Li, Na, K and Ca data were obtained with an aug-pc-3 basis set instead. The electronic configurations tested for negatively charged transition metals obey Hund's maximum multiplicity rule.

	ΔA_{HF} (eV)	ΔA_{MP2} (eV)	ΔA_{exp} (eV)		ΔA_{HF} (eV)	ΔA_{MP2} (eV)	ΔA_{exp} (eV)		ΔA_{HF} (eV)	ΔA_{MP2} (eV)	ΔA_{exp} (eV)
H	-0.3416	0.3435	0.754	Al	0.0211	0.3120	0.434	Mn	-14.3850	-15.5903	0.000
He	-4.7325	-4.6834	0.000	Si	0.8664	1.3126	1.390	Fe	-0.9948	-2.6280	0.153
Li	-0.1234	0.3448	0.618	P	-0.3705	0.2678	0.747	Co	1.0615	-2.7030	0.662
Be	-0.4413	-0.3642	0.000	S	0.9170	1.7980	2.077	Ni	-61.5652	-62.1103	1.157
B	-0.3028	0.1447	0.280	Cl	2.4688	3.5558	3.613	Cu	-0.0057	0.7636	1.236
C	0.4624	1.1876	1.262	Ar	-4.0641	-3.9331	0.000	Zn	-0.6684	-0.6113	0.000
N	-1.8660	-0.7209	0.000	K	-0.0805	0.3317	0.501	Ga	-0.0349	0.2513	0.430
O	-0.5344	1.2737	1.462	Ca	-0.2800	-0.2379	0.024	Ge	0.8818	1.2945	1.233
F	1.2712	3.5488	3.401	Sc	1.2759	1.1630	0.189	As	-0.2943	0.3077	0.814
Ne	-7.9441	-7.8670	0.000	Ti	0.2316	0.3861	0.087	Se	1.0070	1.7814	2.021
Na	-0.1057	0.3331	0.548	V	-2.4207	-4.7335	0.528	Br	2.4928	3.3978	3.364
Mg	-0.4180	-0.3291	0.000	Cr	-4.0782	-5.3915	0.676	Kr	-3.6817	-3.5393	0.000